Gravitational Wave probes for Dark Matter

Antonino Marcianò

Fudan University

Addazi & A. Marciano, IJMPA 2018; A. Addazi, R. Ciancarella, F. Pannarale, A. Marciano
Phys.Dark Univ. 32 (2021) 100796

Lund COST Advanced School on Physics of Dark Matter and Hidden Sectors: from Theory to Experiment, 18-22 September 2021

Plan of the talk

The multi-messenger approach & particle physics

GW generated by FOPT

Neutrino physics and the mass-generation

See-saw mechanism and GW production

Partial conclusions

The multi-messenger approach & particle physics

The multi-messenger approach

Electro-magnetism
Neutrinos
Comic rays
GW signals

Use gravitational waves to probe high and low-scale physics

Ex. : LISA, U-DECIGO and BBO can test SSB in 10 GeV-10 TeV

Ex. : PTA, SKA, FAST (nHz range) can test in MeV-ish scales

Cross-checking strategy: meson factories, LHC, CEPC, etc…

Recurrent questions

What is the nature of Dark Matter?

Can we use Gravitational Waves to unveil its nature?

Can we use a cross-checking multi messenger strategy?

How does neutrinos' mass generate?

Can we understand the nature of the inflaton?

What can we infer about confinement in QCD?

We deploy at the same time informations from different observational channels!

Gravitational Waves

$$g_{\mu\nu} = \eta_{\mu\nu} + h_{\mu\nu}$$

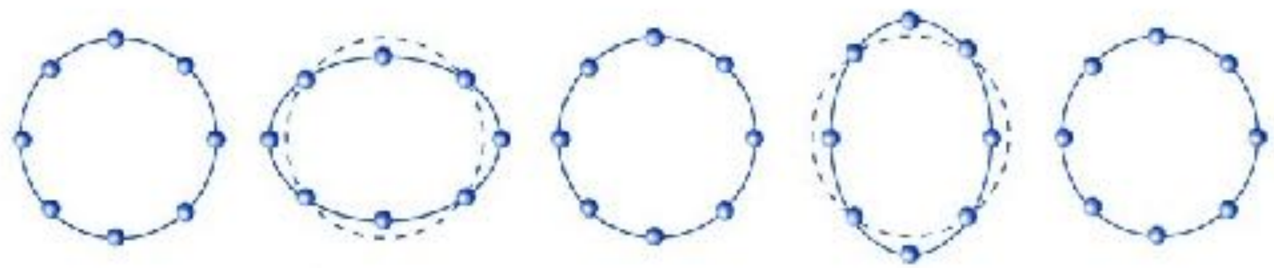

2 propagating d.o.f.

$$\frac{1}{c^2}\frac{\partial^2}{\partial t^2} - \nabla^2 h_{ij}(\mathbf{x},t) = \frac{16\pi G}{c^4} S_{ij}(\mathbf{x},t)$$

$$S_{ij}(\mathbf{x},t) \equiv T_{ij}(\mathbf{x},t) - \frac{1}{3}\delta_{ij} T^k{}_k(\mathbf{x},t)$$

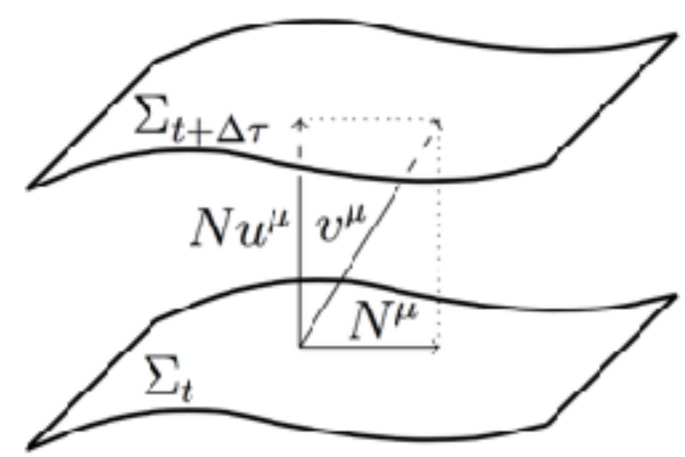

Gravitational Waves

Gravitational Waves

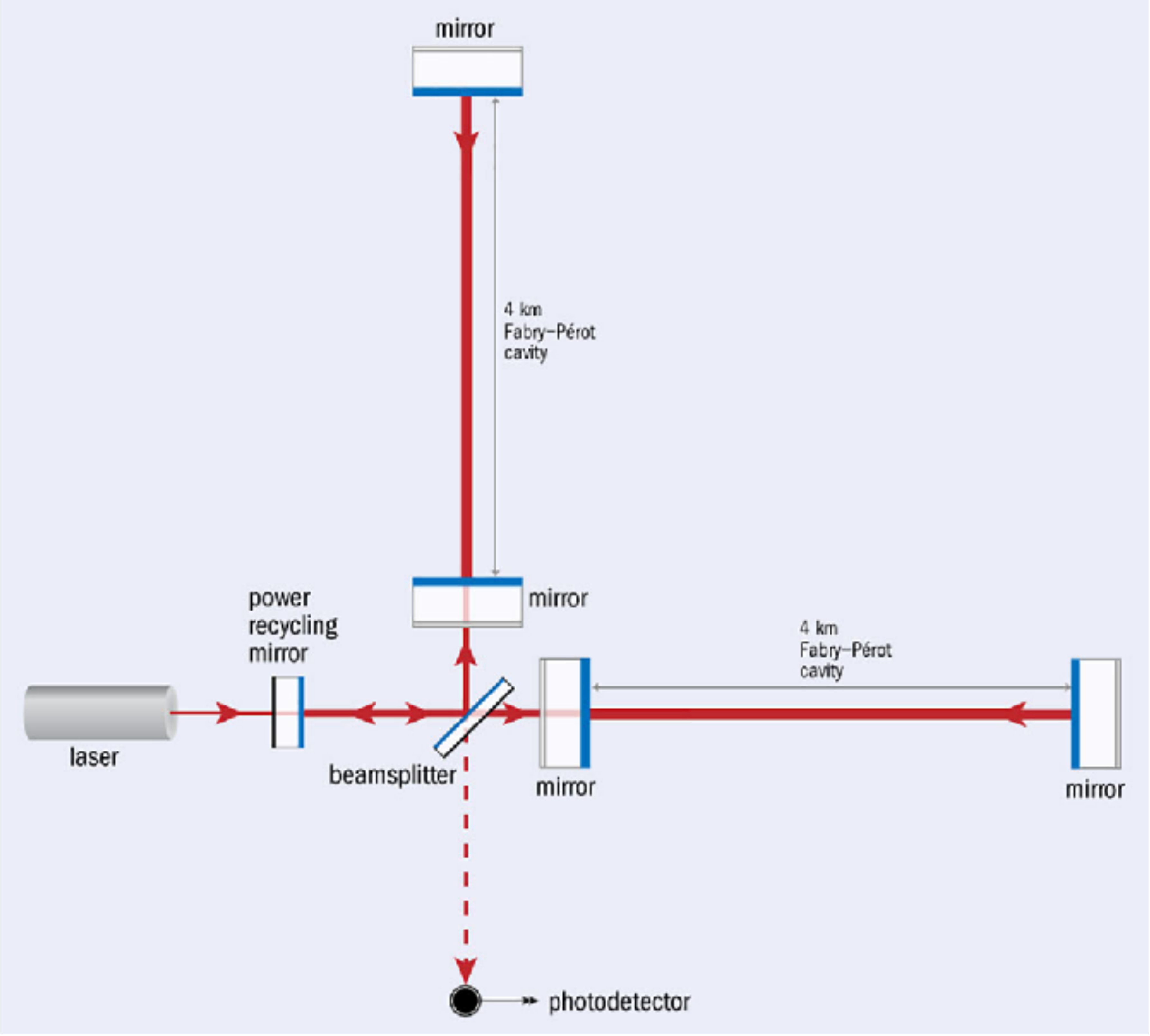

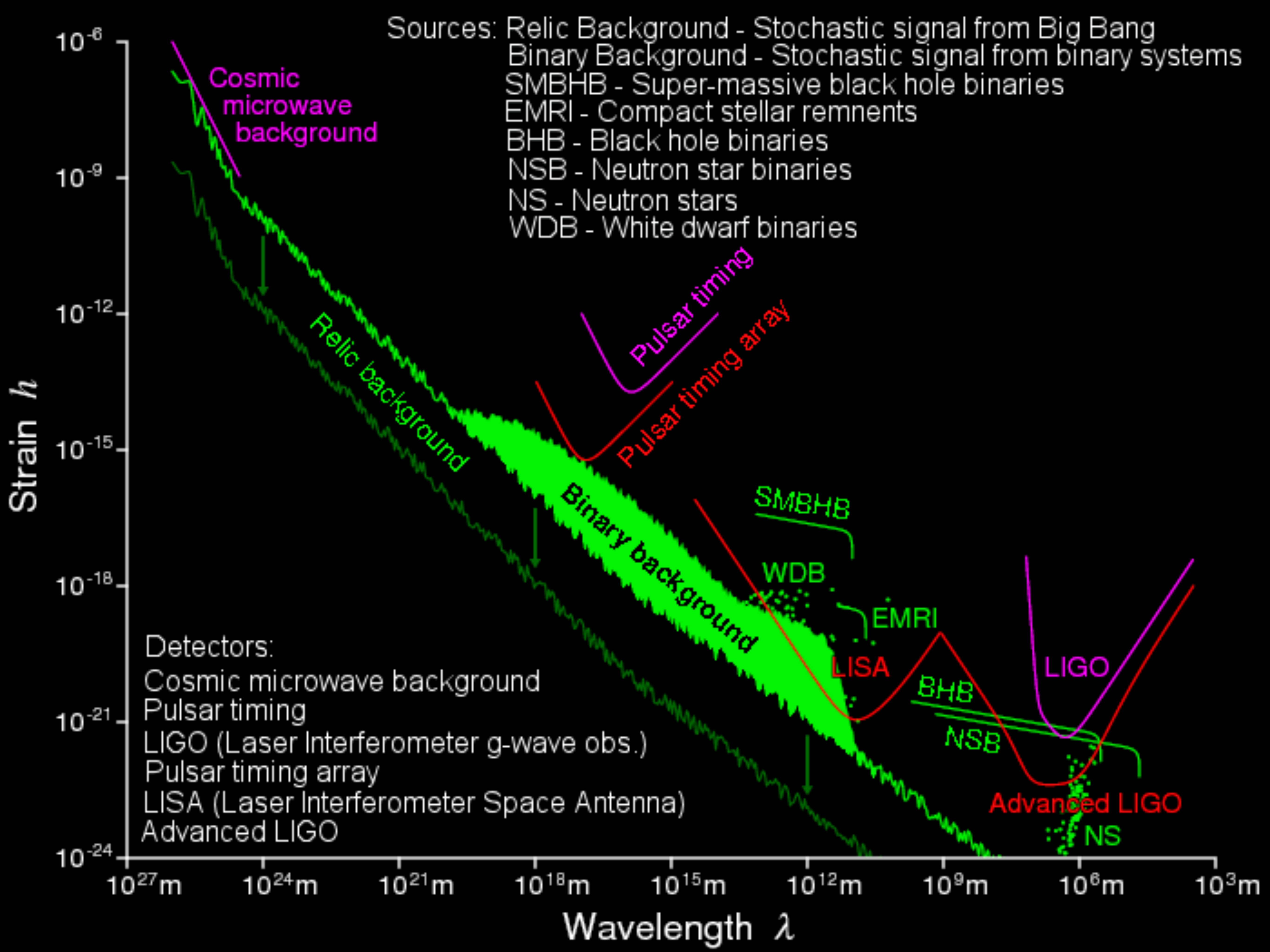
Sources: Relic Background - Stochastic signal from Big Bang
Binary Background - Stochastic signal from binary systems
SMBHB - Super-massive black hole binaries
EMRI - Compact stellar remnents
BHB - Black hole binaries
NSB - Neutron star binaries
NS - Neutron stars
WDB - White dwarf binaries
Cosmic microwave background
Pulsar timing
Pulsar timing array
Relic background
Binary background
SMBHB
WDB
EMRI
LISA
LIGO
BHB
NSB
Advanced LIGO
NS
Detectors:
Cosmic microwave background
Pulsar timing
LIGO (Laser Interferometer g-wave obs.)
Pulsar timing array
LISA (Laser Interferometer Space Antenna)
Advanced LIGO
Strain h
Wavelength λ
10^{-6}
10^{-9}
10^{-12}
10^{-15}
10^{-18}
10^{-21}
10^{-24}
10^{27}m
10^{24}m
10^{21}m
10^{18}m
10^{15}m
10^{12}m
10^{9}m
10^{6}m
10^{3}m

Gravitational Waves

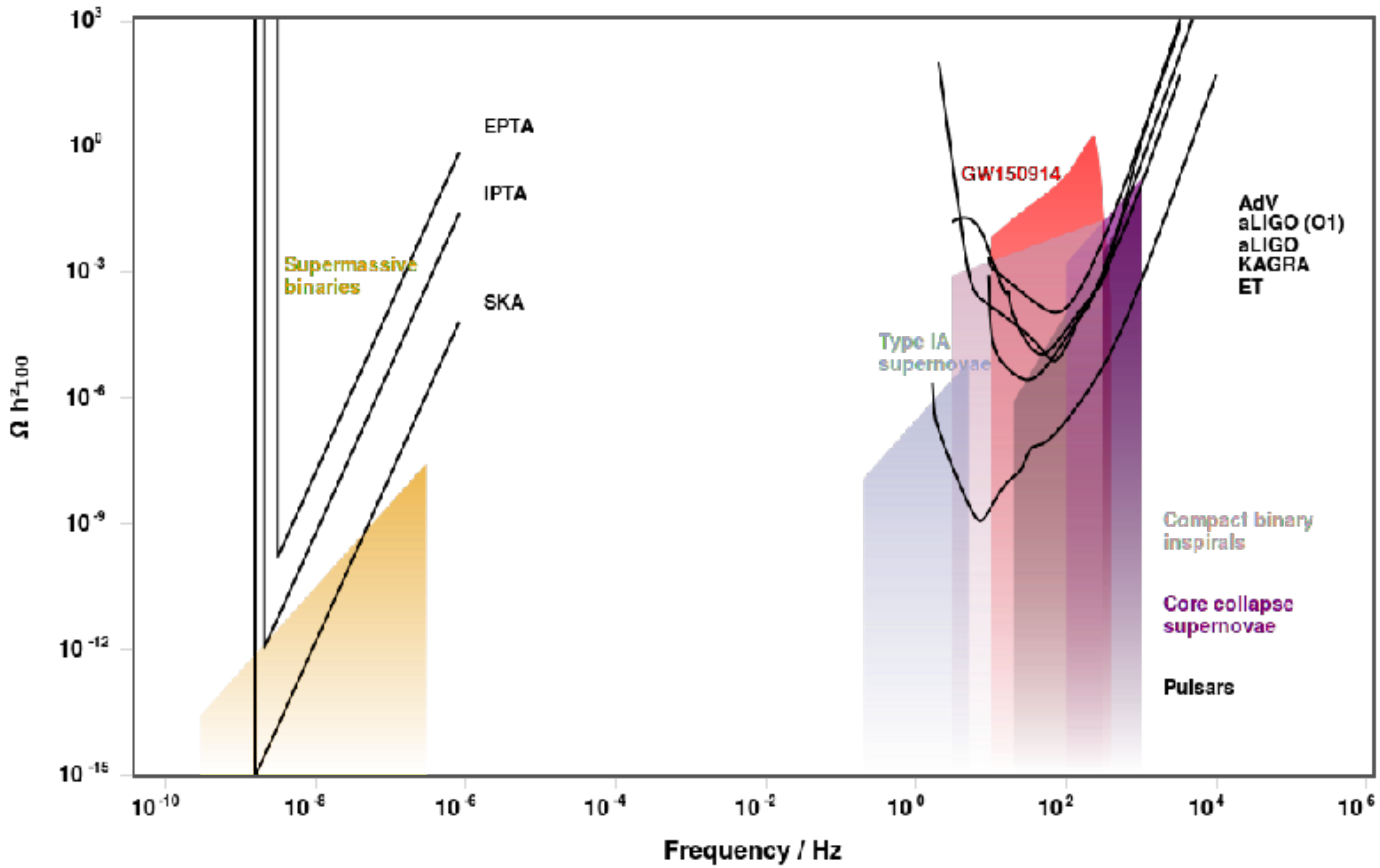

Credit: G. Nardini (Lisa collaboration), Fudan 2017

Gravitational Waves

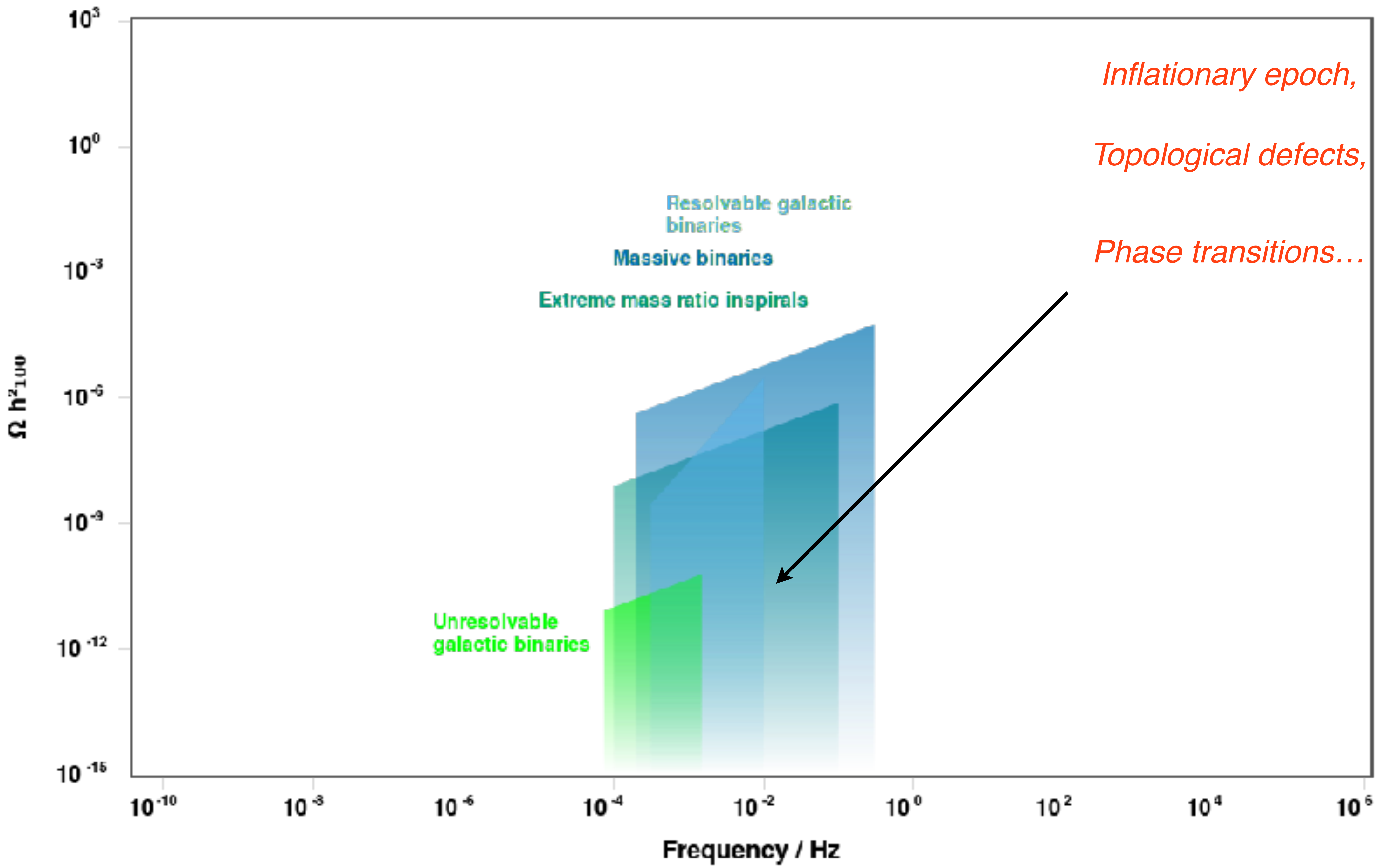

Credit: G. Nardini (Lisa collaboration), Fudan 2017

First observations of Gravitational Waves

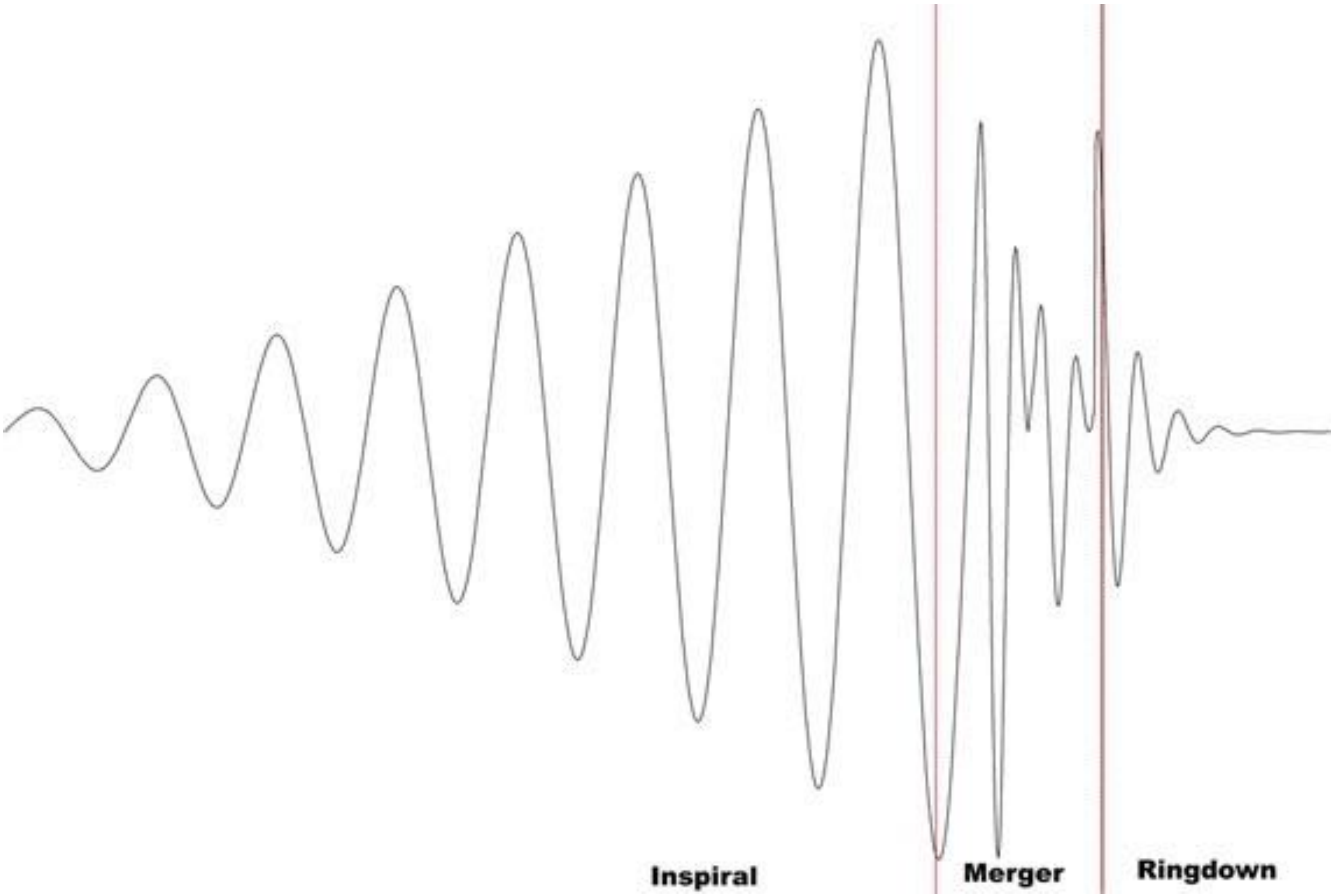

First observations of Gravitational Waves

GW150914

Distance ~ 440 Mpc

~3 solar masses emitted in GW

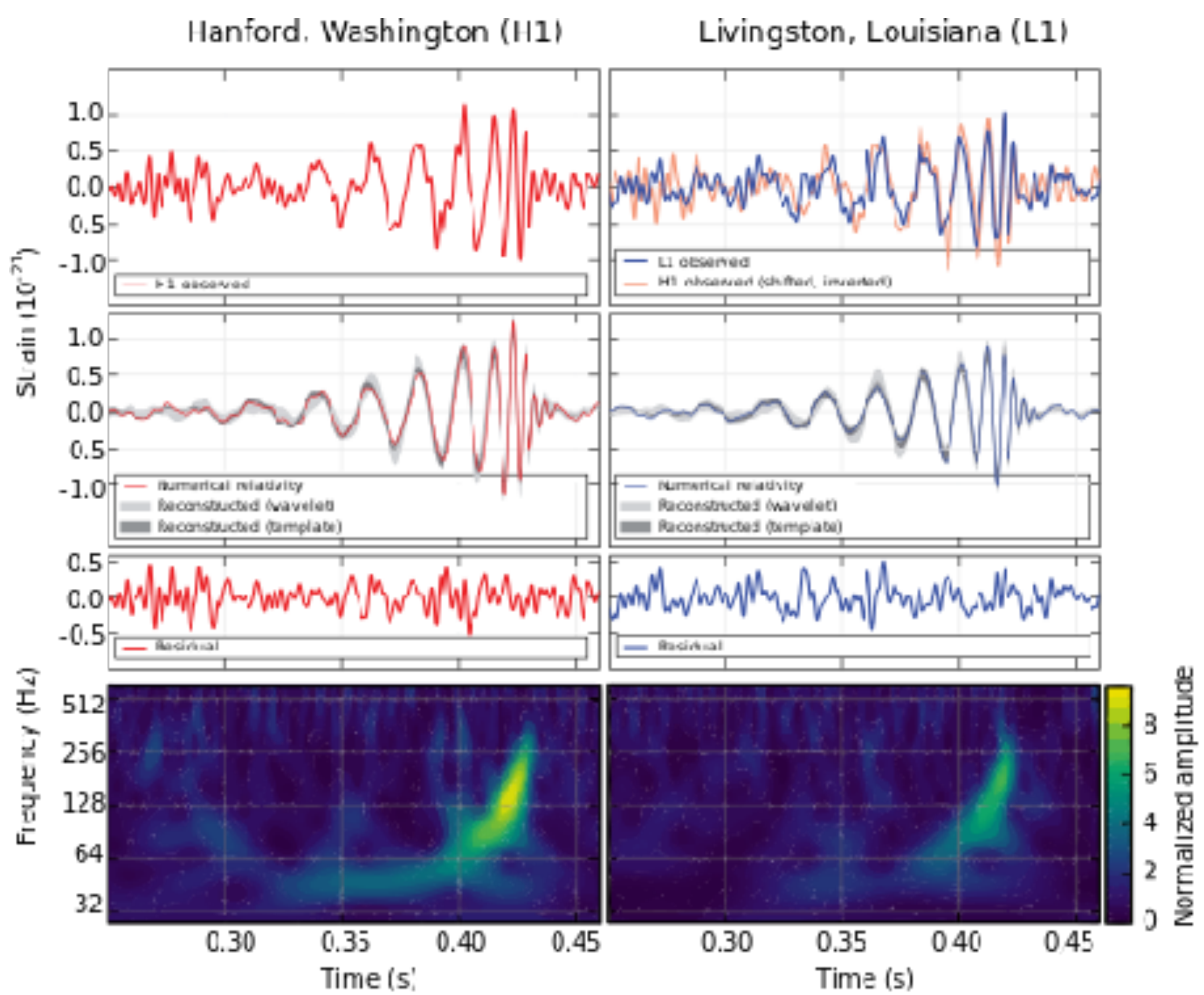

First observations of Gravitational Waves

GW170814

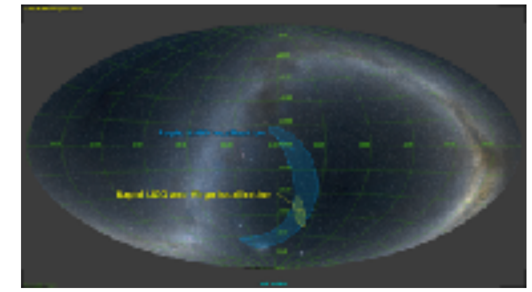

Distance ~ 540 Mpc

~3 solar masses emitted in GW

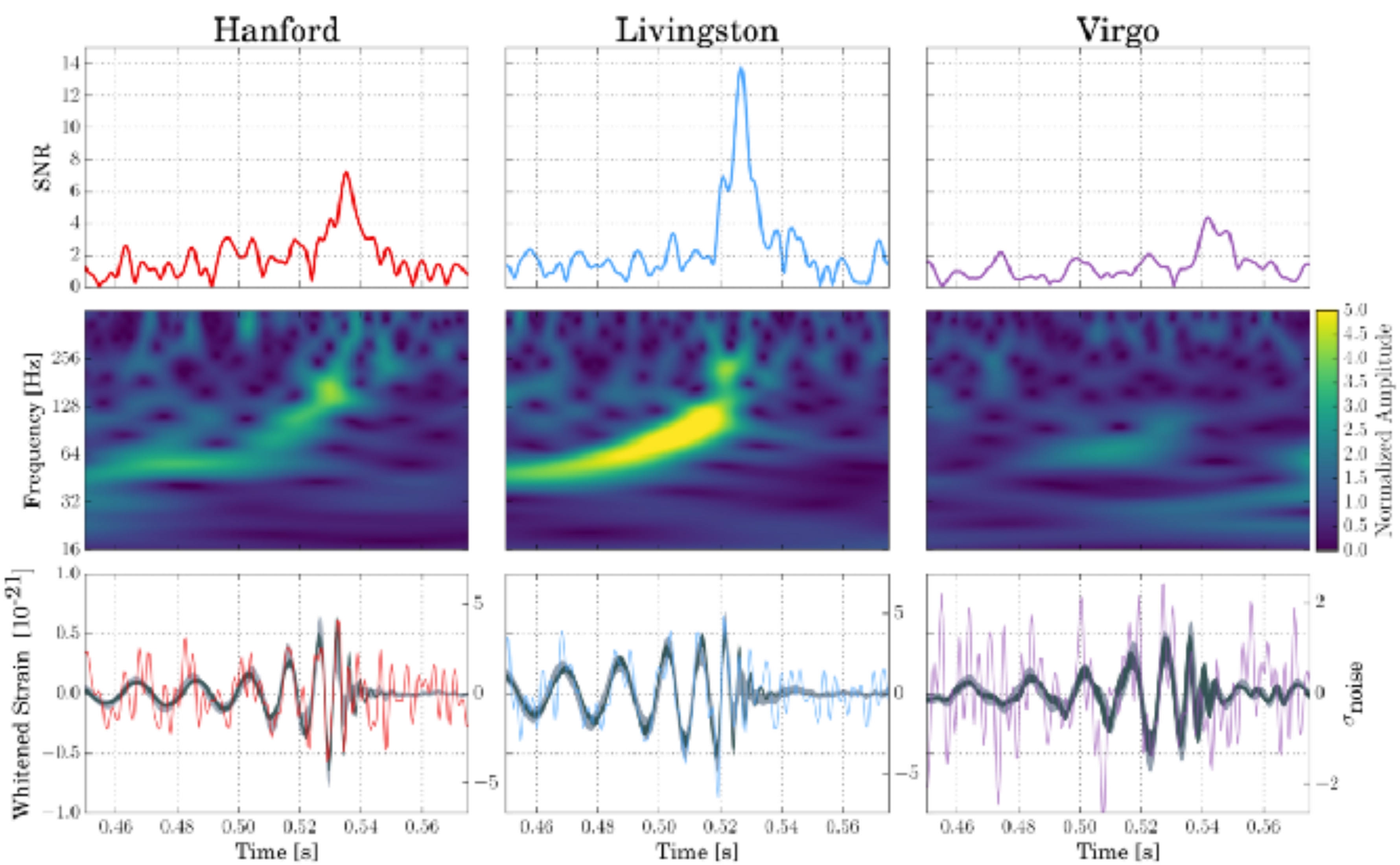

Multi-messenger perspective for Dark Matter

GW170817

GRB170817A

Distance ~ 40 Mpc

Neutron stars around 1 and 2 solar masses

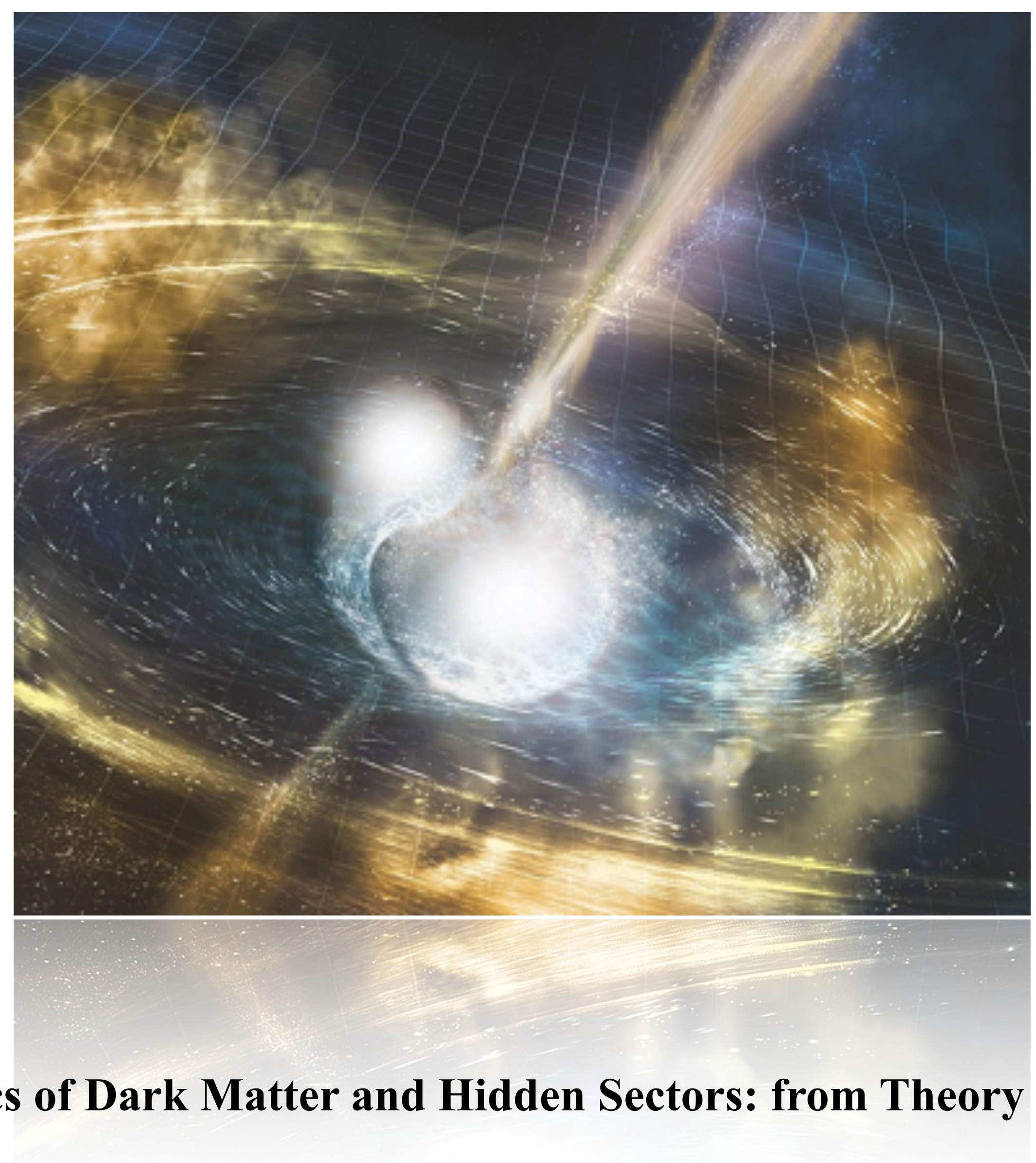

Multi-messenger perspective for Dark Matter

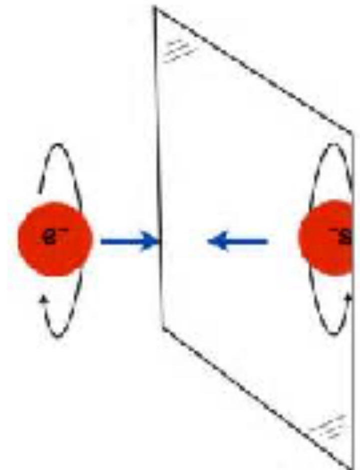

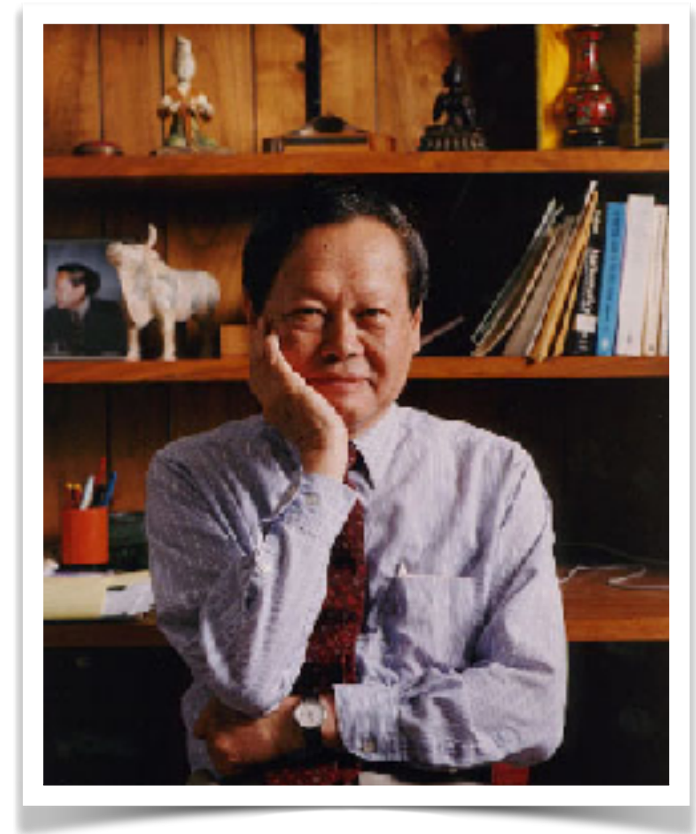

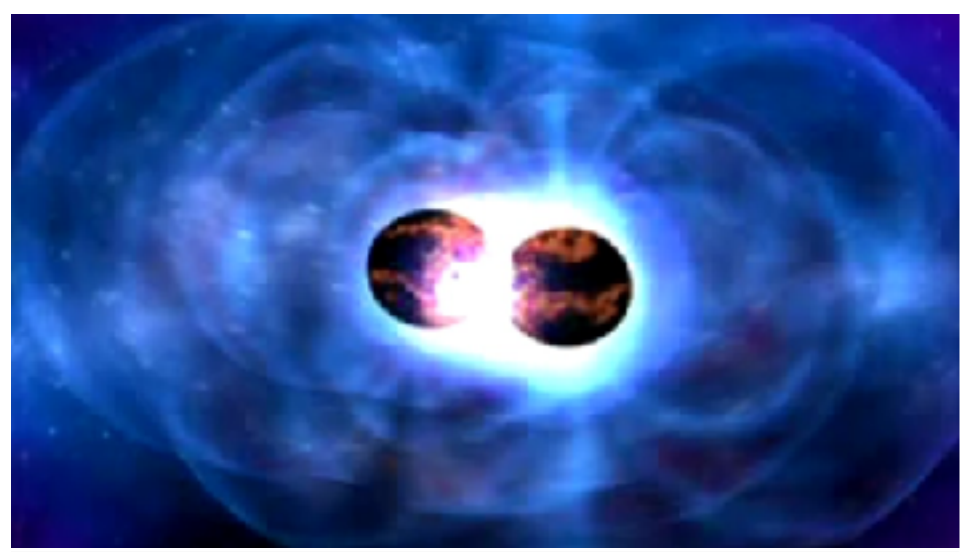

Addazi & A. Marciano, IJMPA 2018; A. Addazi, R. Ciancarella, F. Pannarale, A. Marciano
Phys.Dark Univ. 32 (2021) 100796

Equations of State for Neutron Stars

$$Q_{ij} = -\lambda \varepsilon_{ij}$$

Solve static equilibrium equations (TOV)
and second order differential equations Hinderer (2010)

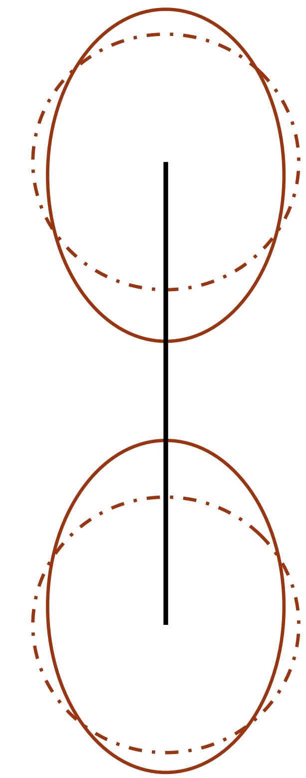

$\Lambda = \frac{\lambda}{M^5}$

$$\Lambda_{GW170817} = 190^{+390}_{-120}$$

Measuring NS deformability $\longrightarrow$ matter in density regimes inaccessible on Earth

Pions presence, nontrivial fluidodynamics… $\longrightarrow$

Anisotropic models

$$p_t(r) = p_r + \frac{\zeta}{3}\frac{r(\varepsilon - 3p_r)}{r - 2m(r)}(\varepsilon - p_r)r^2$$

Bowers & Liang 1974

Static equilibrium and TOV

$$T^{\alpha}_{\beta} = Diag(\varepsilon, p, p, p)$$

$$ds^2 = -e^{2\Phi}dt^2 + e^{2\Lambda}dr^2 + r^2 d\theta^2 + r^2(\sin\theta)^2 d\phi^2$$

$$G_{\alpha\beta} = 8\pi T_{\alpha\beta}$$

$$\nabla_{\alpha} T^{\alpha\beta} = 0$$

$$\begin{cases} e^{-2\Lambda} = 1 - \dfrac{2m(r)}{r} \\ \dfrac{d\Phi}{dr} = \dfrac{1}{r} e^{2\Lambda}\left[8\pi^2 p(r) + \dfrac{2m(r)}{r}\right] \\ \dfrac{dp}{dr} = -\big(p(r) + \varepsilon(r)\big)\dfrac{d\phi}{dr} \end{cases}$$

System is closed by an EoS: $p = p(\varepsilon)$

Role of anisotropies in NS EoS I

A. Addazi, R. Ciancarella, A. Marciano & F. Pannarale *Phys.Dark Univ.* 32 (2021) 100796

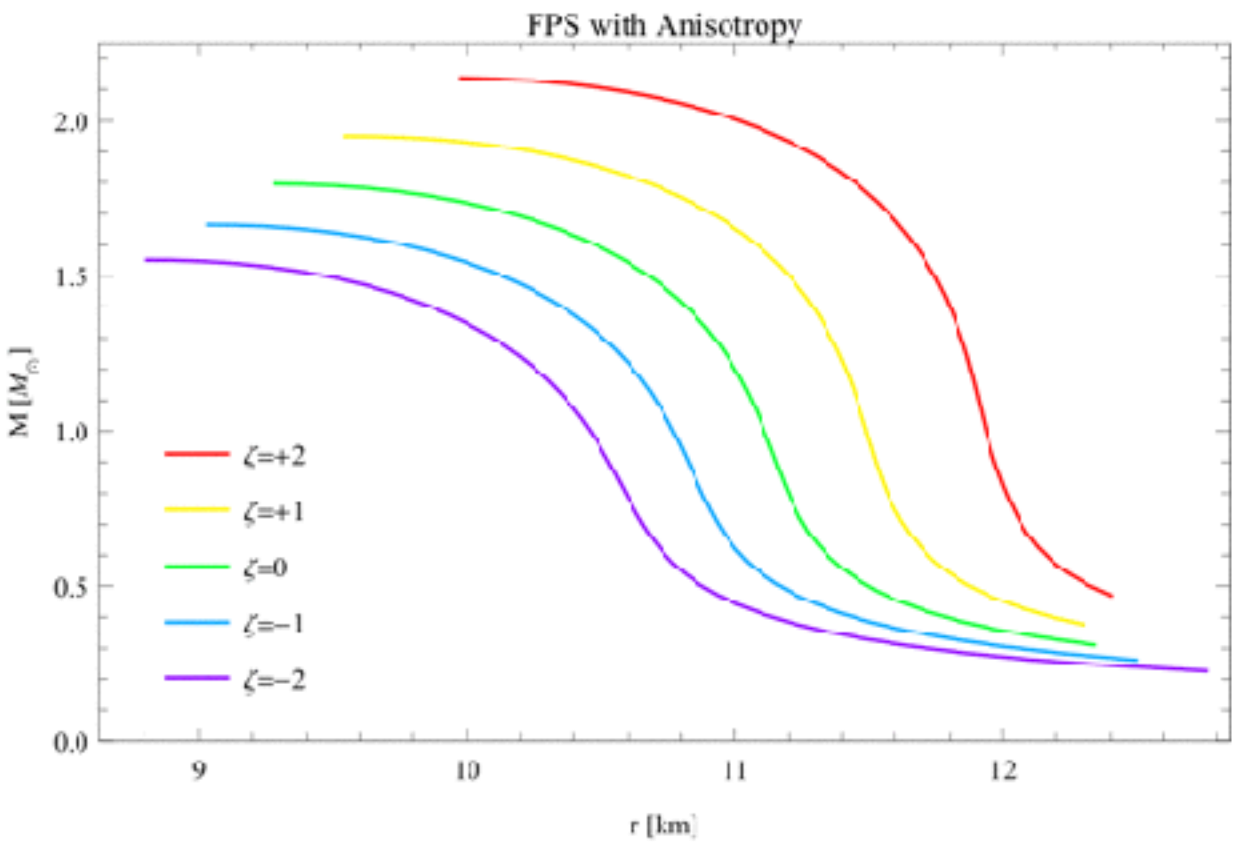

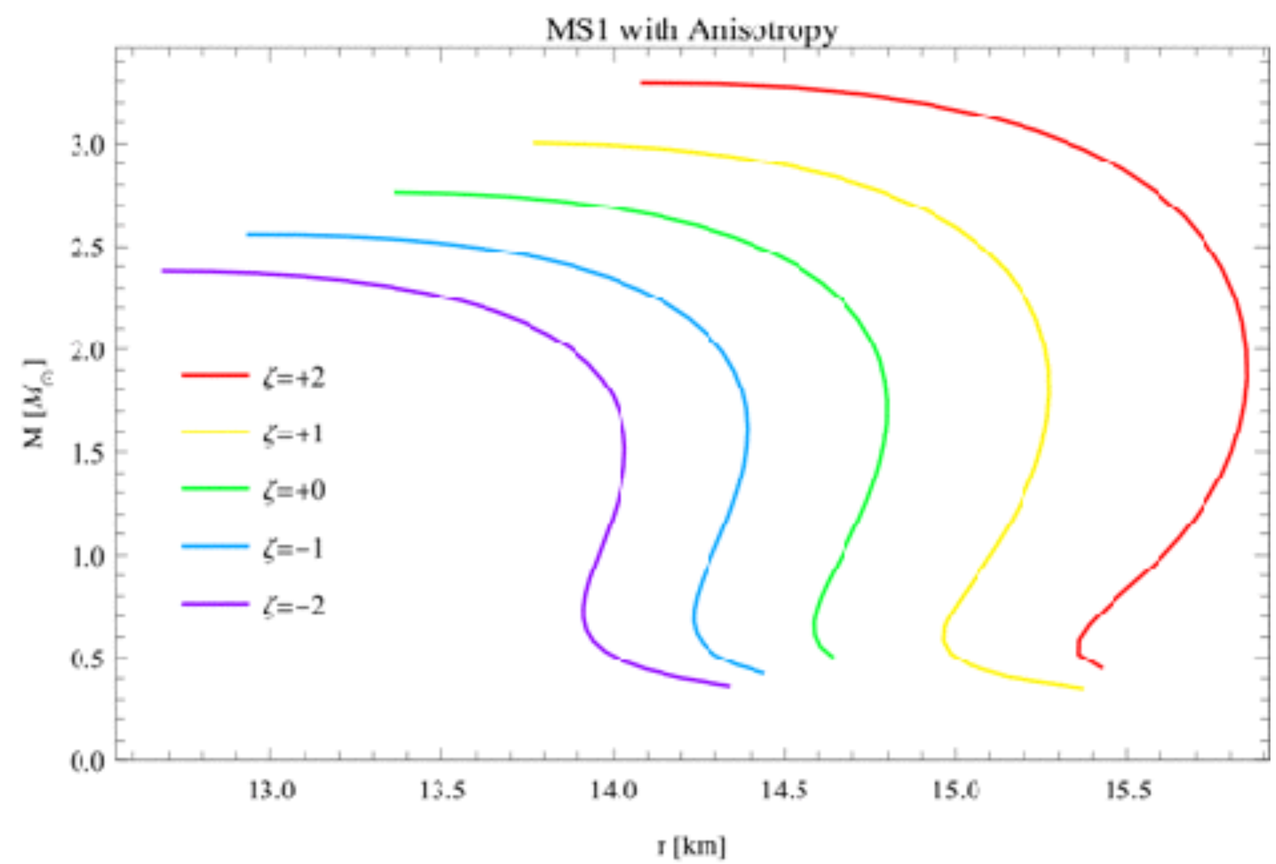

FPS

	$\zeta = +2$	$\zeta = +1$	$\zeta = -1$	$\zeta = -2$
R(km)	11.80	11.29	10.36	9.86
C	0.175	0.183	0.200	0.210
k_2	0.0863	0.0741	0.0577	0.0511
$\lambda(10^{36}\,\mathrm{g\,cm^2\,s^2})$	1.97	1.36	0.69	0.48

MS1

	$\zeta = +2$	$\zeta = +1$	$\zeta = -1$	$\zeta = -2$
R(km)	15.78	15.23	14.38	14.03
C	0.131	0.136	0.144	0.147
k_2	0.130	0.114	0.0904	0.0842
$\lambda(10^{36}\,\mathrm{g\,cm^2\,s^2})$	12.7	9.31	5.55	4.57

Role of anisotropies in NS EoS II

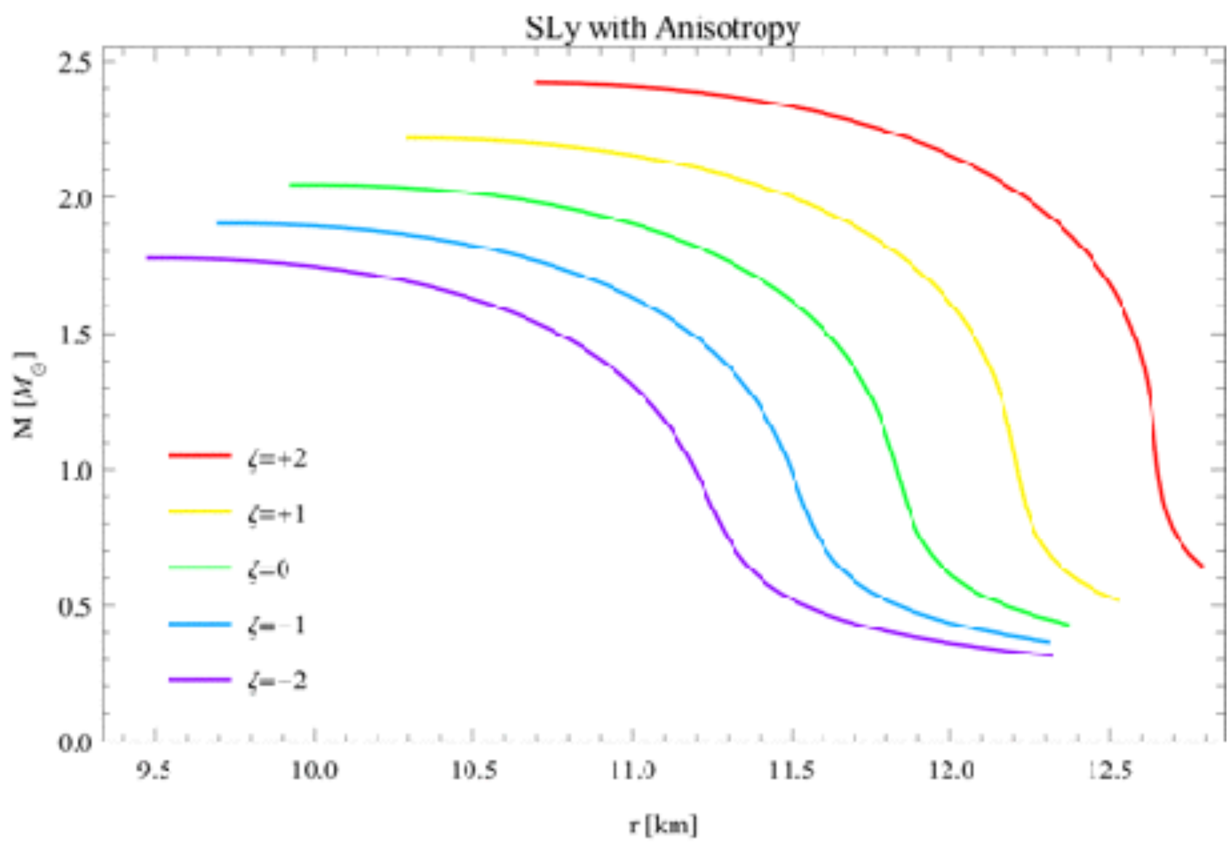

SLy

	$\zeta = +2$	$\zeta = +1$	$\zeta = -1$	$\zeta = -2$
R(km)	12.60	12.11	11.28	10.91
C	0.164	0.171	0.183	0.190
k_2	0.0952	0.0829	0.0663	0.0608
$\lambda(10^{36}\ \mathrm{g\,cm^2\,s^2})$	3.02	2.16	1.21	0.93

ζ>0

Maximal mass at fixed central pressure increases.
Tidal deformability increases while compactness decreases.

ζ<0

Maximal mass at fixed central pressure decreases.
Tidal deformability decreases while compactness increases.

Mirror Dark Matter I

Following T.D. Lee & C. Yang (1956), parity, as a global symmetry, might be restored in a dark sector:

- *The Dark Sector as copy of the Standard Model, with opposite chirality*
- *Different nucleosynthesis*
- *Interacting either gravitationally or weakly coupled to EM*

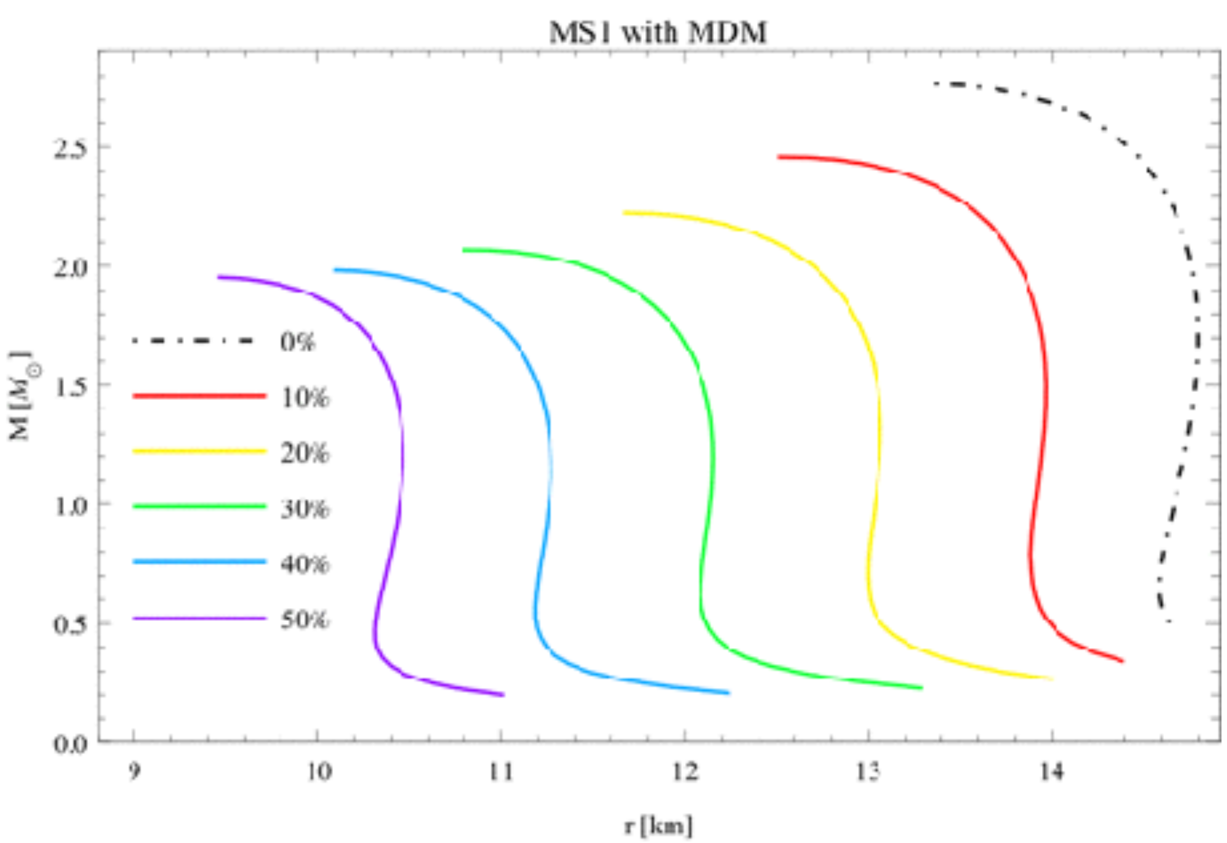

0%<MDM<50%

Maximal mass decreases at fixed central pressure.
Tidal deformability decreases while compactness increases.

MDM>50%

Specular to the case above

MS1 with MDM

	10%	20%	30%	40%	50%
R(km)	13.97	13.06	12.13	11.24	10.44
C	0.148	0.158	0.170	0.184	0.198
k_2	0.0838	0.0737	0.0647	0.0623	0.0676
$\lambda(10^{36}\,\mathrm{g\,cm^2\,s^2})$	4.44	2.80	1.70	1.12	0.839

Mirror Dark Matter II

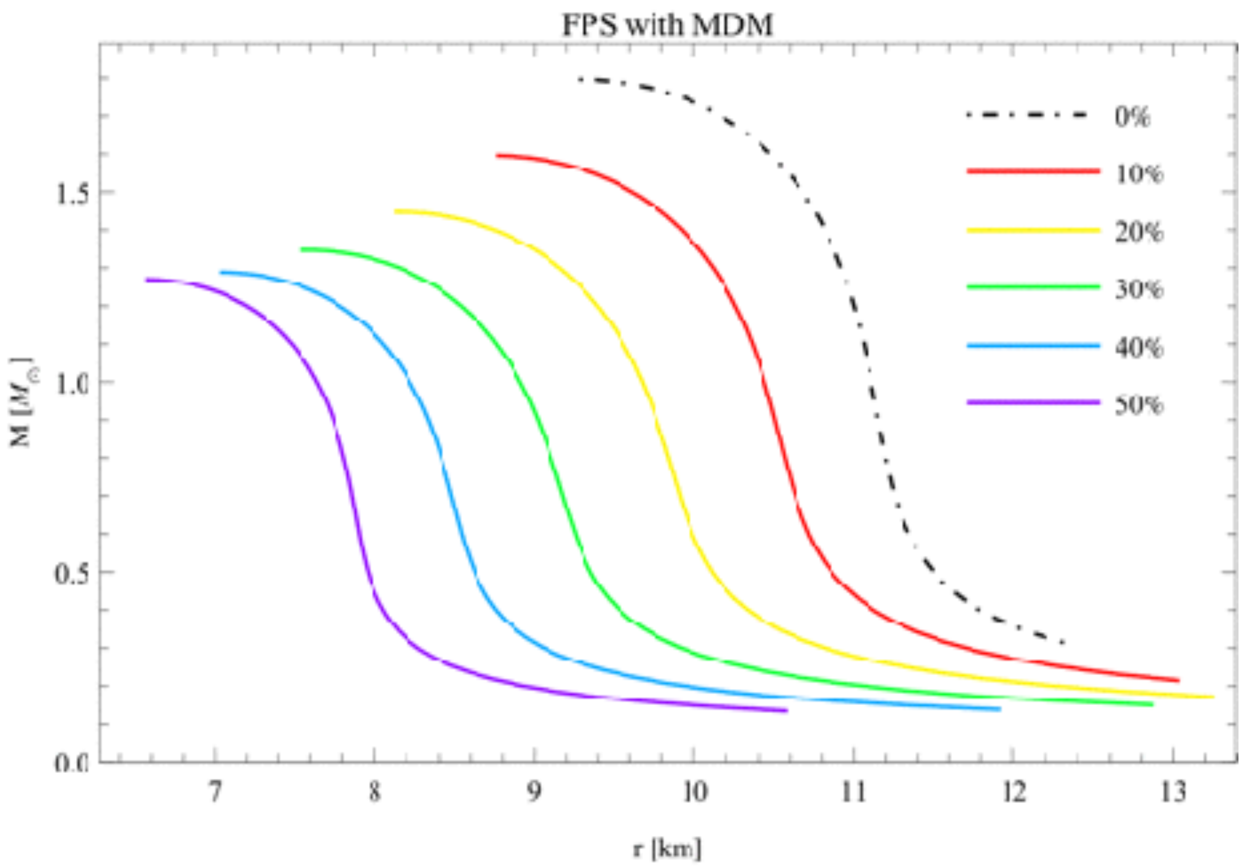

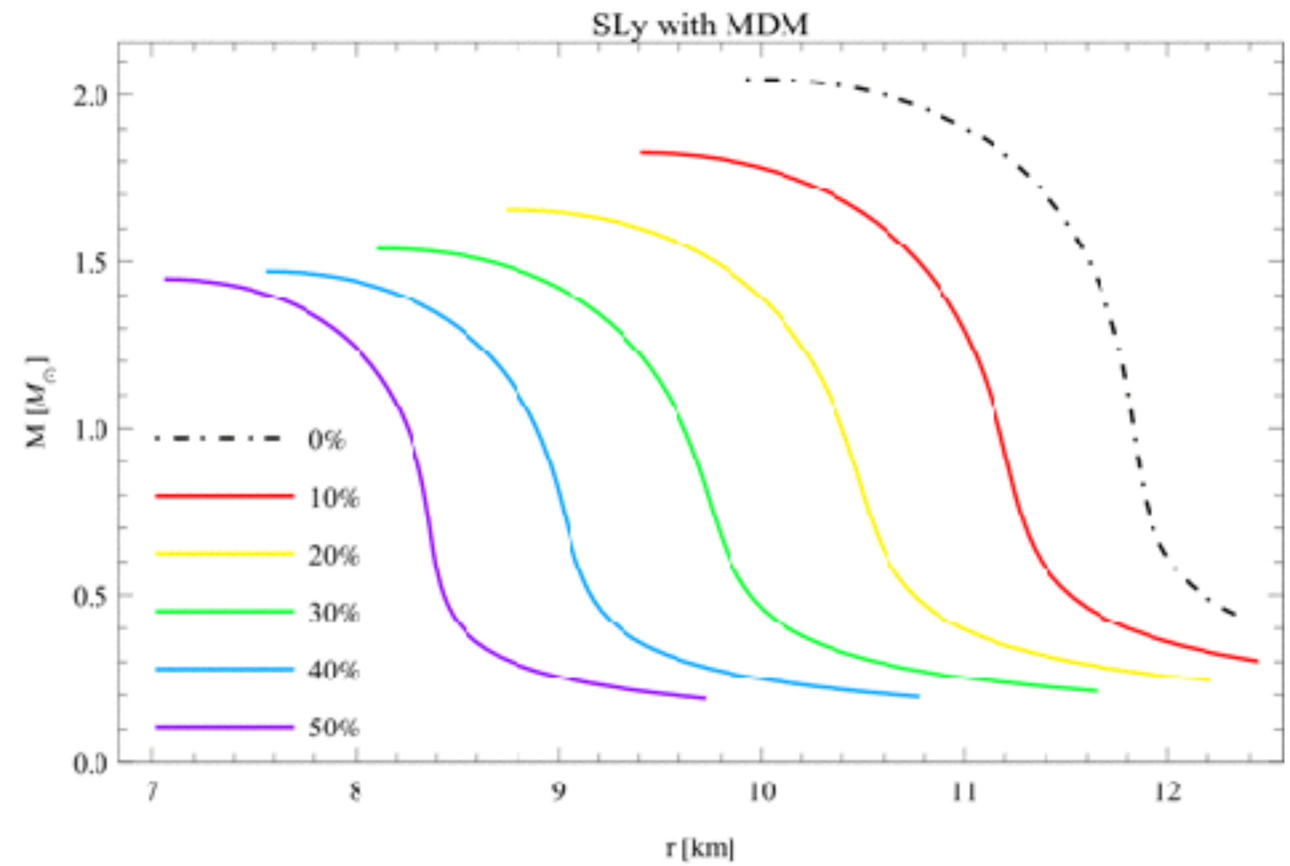

FPS with MDM

	10%	**20%**	**30%**	**40%**	**50%**
R (km)	10.36	9.56	8.76	8.06	7.47
C	0.157	0.170	0.185	0.202	0.217
k_2	0.0724	0.0605	0.0535	0.0508	0.0523
$\lambda\,(10^{36}\,\mathrm{g\,cm^2\,s^2})$	0.865	0.482	0.276	0.172	0.124

SLy with MDM

	10%	**20%**	**30%**	**40%**	**50%**
R(km)	10.90	9.98	9.06	8.22	7.57
C	0.190	0.207	0.228	0.251	0.273
k_2	0.0600	0.0485	0.0404	0.0352	0.0333
$\lambda(10^{36}\,\mathrm{g\,cm^2\,s^2})$	0.921	0.481	0.247	0.132	0.0831

Confronting with GW170817 and PSR J0349+4032

Inferred Mass from PSR J0348+4032

$$M = (1.97 \div 2.05) M_{\odot}$$

% of MDM	0%	10%	20%	30%	40%	50%
SLy	**282**	163	85	44	23	15
MS1	1246	786	**495**	**301**	**197**	148

Tidal deformability from GW170817

$$\Lambda_{GW170817} = 190^{+390}_{-120}$$

$$\Lambda = \frac{\lambda}{M^5}$$

ζ	+2	+1	0	-1	-2
FPS	**349**	240	172	121	84
SLy	**534**	**381**	**282**	214	165
~~MS1~~	~~2242~~	~~1645~~	~~1246~~	~~979~~	~~807~~

Necessary condition

Given either the families EoS-ζ or EoS-MDM, there must be a sequence that satisfies PSR J0348+4032 and a sequence that satisfies GW170817

Within the range assumed:

a) MS1 is rejected for the anisotropic case
b) FPS is rejected in the MDM case

Confronting with GW170817 and PSR J0349+4032

Inferred Mass from PSR J0348+4032

$M = (1.97 \div 2.05) M_{\odot}$

% of MDM	0%	10%	20%	30%	40%	50%
SLy	**282**	163	85	44	23	15
MS1	1246	786	**495**	**301**	**197**	148

Tidal deformability from GW170817

$\Lambda_{GW170817} = 190^{+390}_{-120}$

$\Lambda = \frac{\lambda}{M^5}$

ζ	+2	+1	0	-1	-2
FPS	**349**	240	172	121	84
SLy	**534**	**381**	**282**	214	165
MS1	2242	1645	1246	979	807

Sufficient condition

Given either the families EoS-ζ or EoS-MDM, there must be at least a sequence satisfying at the same time PSR J0348+4032 e GW170817

Future perspective on NS EoS and (M)DM

Anisotropies

Several configurations EoS-ζ satisfy constraints separately. Other satisfy both the constraints

MS1 is rejected in the anisotropic case

FPS must be reconsidered, since it turns out that it can still be valid

Mirror Dark Matter

Several configurations EoS-ζ satisfy constraints separately. Other satisfy both the constraints

FPS is rejected in presence of MDM.

MS1 must be reconsidered, since it turns out that can be still valid.

Recover tidal deformability for different EoS

Implement different model of dark matter

Develop template for wave-forms

Confrontation with the EM channel!

GW generated by FOPT

Gravitational Waves Stochastic Background

Signal from unresolved astrophysical sources

Signal from cosmological events

i) Early cosmology (inflation, bouncing cosmologies, string gas cosmology etc…)

ii) Cosmic strings

iii) Strong Cosmological Phase Transitions

Tunnelling and bubbles enucleation

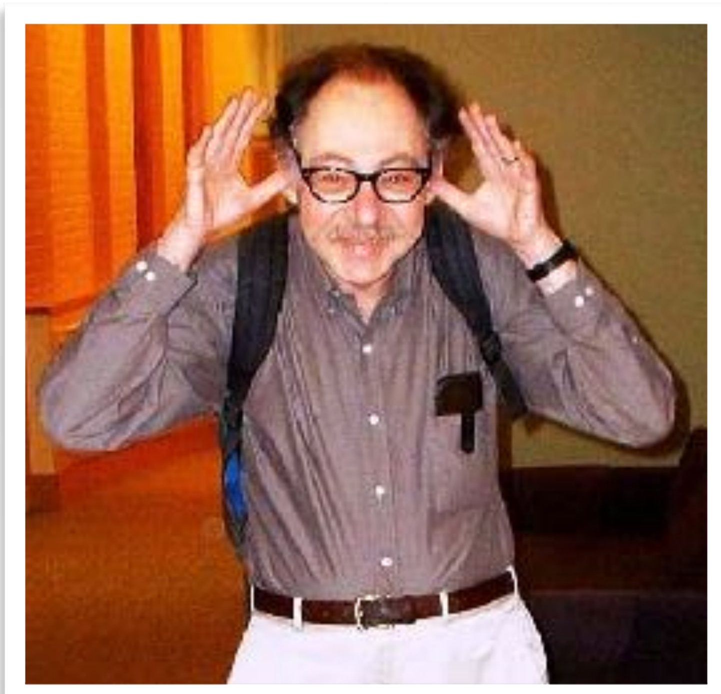

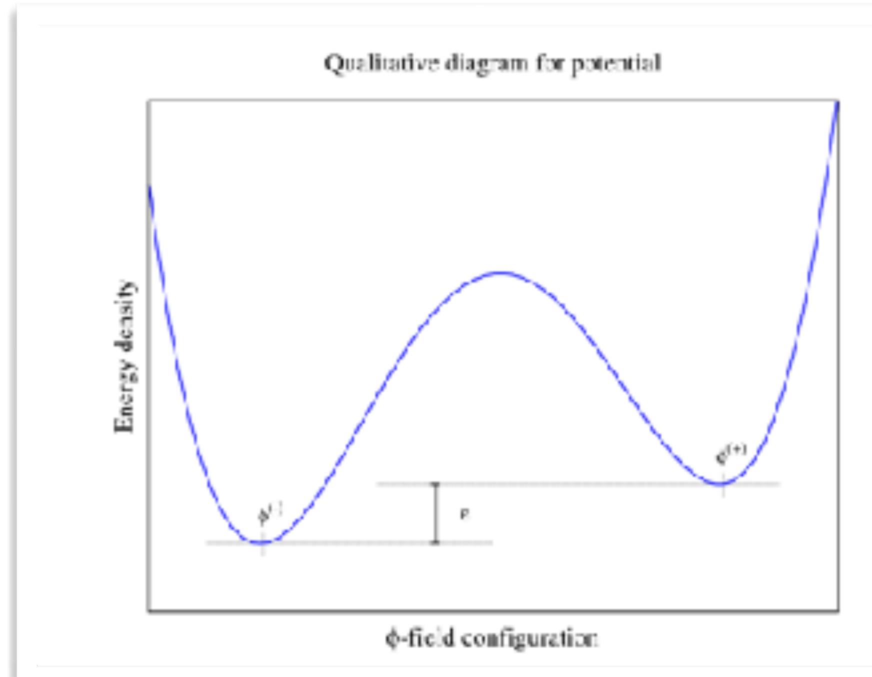

Coleman, Frampton etc…

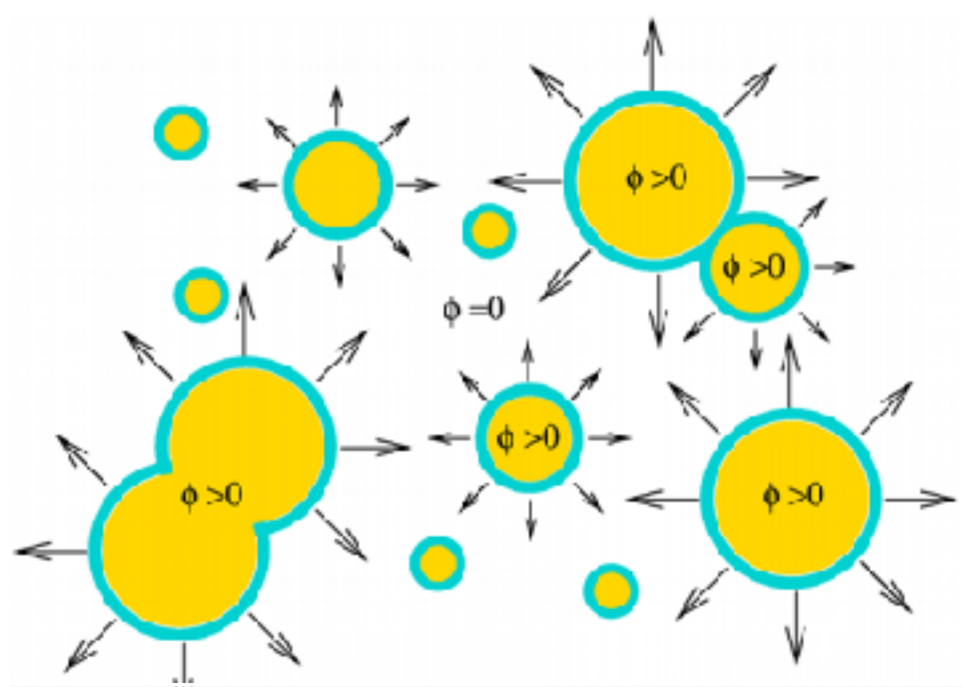

Latent energy parameter

Normalized difference between minima

$$\mathcal{E}(\bar{T}) = \left[T \frac{dV_{eff}}{dT} - V_{eff}(T) \right]_{T=\bar{T}}$$

$$\alpha = \frac{\mathcal{E}(\bar{T})}{\rho_{rad}(\bar{T})} \qquad \rho_{rad} = \frac{\pi^2}{30} g_*(T) T^4$$

Latent Energy

Bubble nucleation parameter

How fast the minimum goes down

$$\beta = -\left[\frac{dS_E}{dt}\right]_{t=\bar{t}} \simeq \left[\frac{1}{\Gamma}\frac{d\Gamma}{dt}\right]_{t=\bar{t}},$$

$$S_E(T) \simeq \frac{S_3(T)}{T} \qquad \Gamma = \Gamma_0(T)\exp[-S_E(T)]$$

$$\Gamma_0(T) \sim T^4, \;\; S_3 \equiv \int d^3r\left(\partial_i s^\dagger \partial_i s + V_{eff}(s,T)\right)$$

β/H provides an inverse time scale

Effective action

Relation between size of the bubble wall and bubble velocity

$$d \simeq \frac{V_B}{\beta}$$

Effective potential

$$\boxed{\begin{gathered} V_{tree}(s, T=0) + V_1(s,T) \\ V_1(s,T) = V_{CW}(s, T=0) + \Delta V(s,T) \end{gathered}}$$

Bubbles collision

$$\nu_{collision} \simeq 3.5 \times 10^{-4} \left(\frac{\beta}{H_*}\right) \left(\frac{\bar{T}}{10\,\mathrm{GeV}}\right) \left(\frac{g_*(\bar{T})}{10}\right)^{1/6} \mathrm{mHz}$$

frequency is proportional to temperature

$$\Omega_{collision}(\nu_{collision}) \simeq C\mathcal{E}^2 \left(\frac{\bar{H}}{\beta}\right)^2 \left(\frac{\alpha}{1+\alpha}\right)^2 \left(\frac{V_B^3}{0.24+V_B^3}\right) \left(\frac{10}{g_*(\bar{T})}\right)$$

$$C \simeq 2.4 \times 10^{-6}$$

corresponding intensity

$h^2\Omega$col dominates for large wall velocities $v_b \to 1$

$$h^2\Omega\left(f;\alpha,\beta/H,f_{\mathrm{peak}}\right) \qquad f_{\mathrm{peak}}\left(\alpha,\beta/H,T_n\right)$$

Shock waves and turbulence

$$f_{\mathrm{SW}}[\mathrm{Hz}] = 1.9 \times 10^{-5} \frac{\beta}{H} \frac{1}{v_b} \left(\frac{T_n}{100\,\mathrm{GeV}} \right) \left(\frac{g_*}{100} \right)^{1/6}$$

$$f_{\mathrm{MHD}}[\mathrm{Hz}] = 2.7 \times 10^{-5} \frac{\beta}{H} \frac{1}{v_b} \left(\frac{T_n}{100\,\mathrm{GeV}} \right) \left(\frac{g_*}{100} \right)^{1/6}$$

frequency is proportional to temperature

$$h^2 \Omega_{\mathrm{SW}}(f) = 2.65 \times 10^{-6} \left(\frac{\beta}{H} \right)^{-1} \left(\frac{\kappa_v \alpha}{1+\alpha} \right)^2 \left(\frac{g_*}{100} \right)^{-1/3} v_b \left(\frac{f}{f_{\mathrm{SW}}} \right)^3 \left(\frac{7}{4 + 3(f/f_{\mathrm{SW}})^2} \right)^{7/2}$$

$$h^2 \Omega_{\mathrm{MHD}}(f) = 3.35 \times 10^{-4} \left(\frac{\beta}{H} \right)^{-1} \left(\frac{\kappa_{\mathrm{turb}} \alpha}{1+\alpha} \right)^{3/2} \left(\frac{g_*}{100} \right)^{-1/3} v_b \left(\frac{f}{f_{\mathrm{MHD}}} \right)^3 \left(\frac{(1 + f/f_{\mathrm{MHD}})^{-11/3}}{1 + 8\pi f / h_*} \right)$$

corresponding intensity

Velocity enhancement

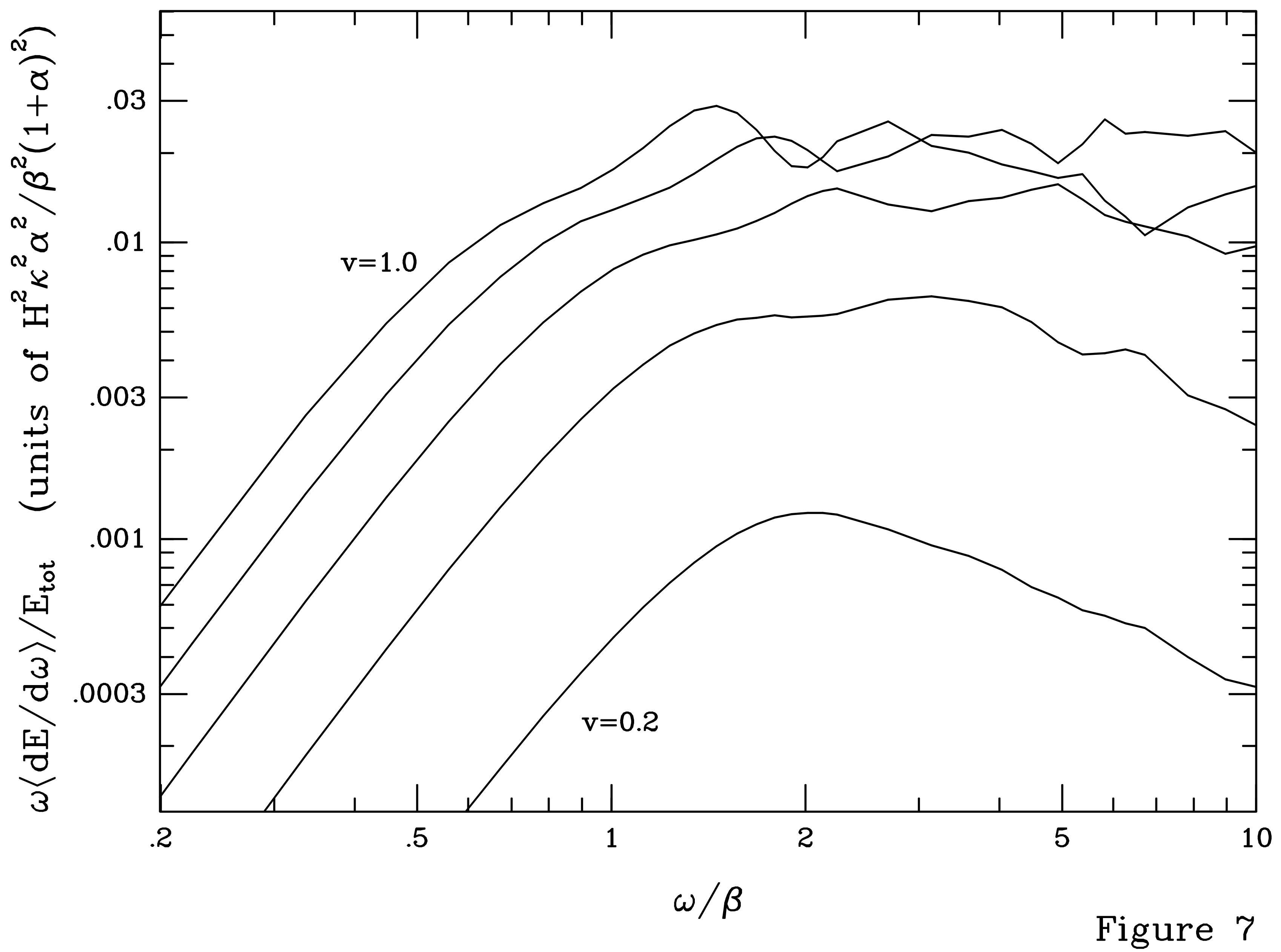

Kamionkowski, Kosowsky, Turner 1994

Credit: A. Kosowsky, Fudan Spring School of Cosmology 2017

Comparison with MHD turbulence

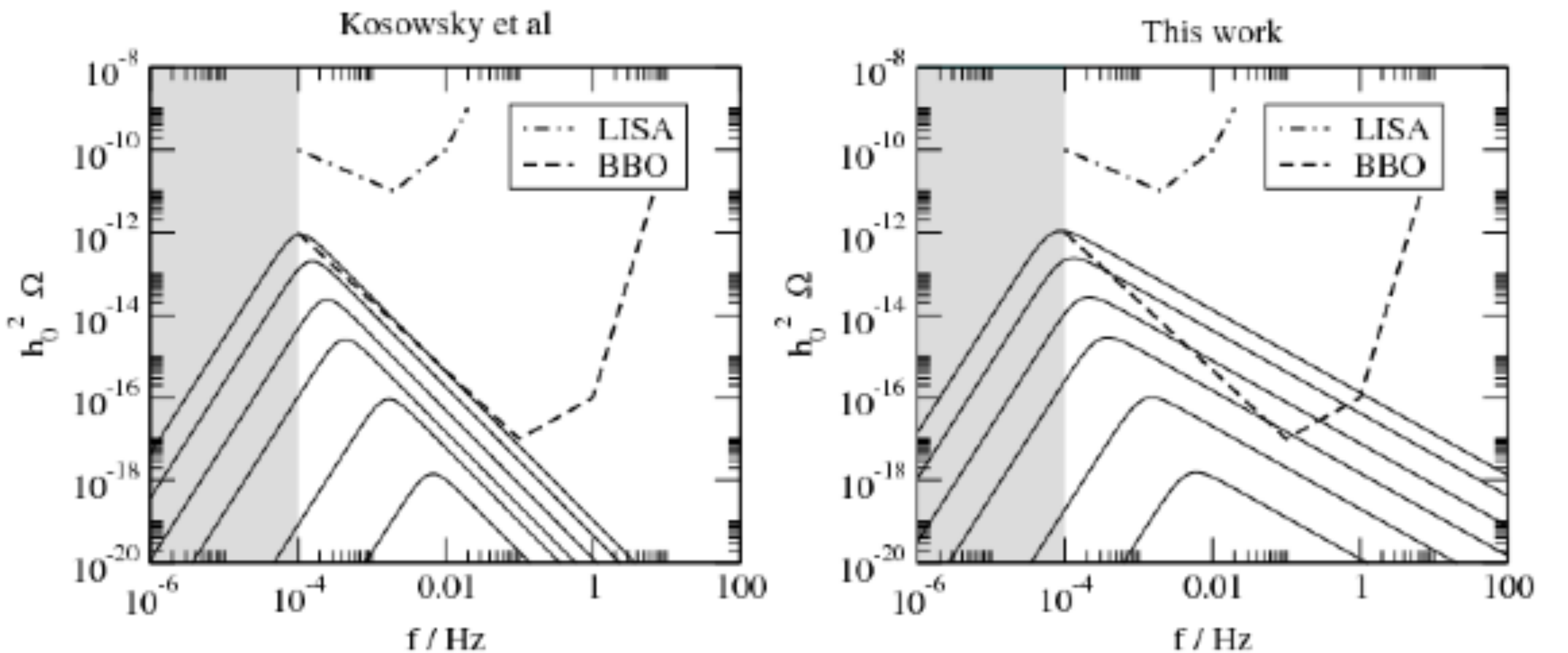

S. Huber, T. Konstandin 2008

Criteria for phase transitions I

Vacuum bubbles nucleated from first order phase transitions (FOPT)

Three sources of GW production: 1) collision, 2) sound waves and 3) plasma turbulence

$h^2\Omega_{\rm col}$ dominates for large wall velocities $v_b \to 1$

$$h^2\Omega\left(f;\alpha,\beta/H,f_{\rm peak}\right) \qquad f_{\rm peak}\left(\alpha,\beta/H,T_n\right)$$

$$\alpha \propto \frac{1}{T_n^4}\left[V_i - V_f - T\left(\frac{\partial V_i}{\partial T} - \frac{\partial V_f}{\partial T}\right)\right] \qquad \frac{\beta}{H} = T_n \frac{\partial}{\partial T}\left(\frac{\hat{S}_3}{T}\right)\bigg|_{T_n}$$

Criteria for phase transitions II

Bubble nucleation arises when the probability to realize 1 transition per cosmological horizon is equal to one: $\frac{\Gamma}{H^4} \sim 1 \Rightarrow \frac{\hat{S}_3}{T_n} \sim 140$

Strong transition criterion: $\frac{v_h(T_n)}{T_n} \geq 1 \Rightarrow$ enhances GW production

Classical motion in Euclidean space described by action $\hat{S}^3$

$$\hat{S}_3 = 4\pi \int_0^\infty \mathrm{d}r\, r^2 \left\{ \frac{1}{2} \left(\frac{\mathrm{d}\hat{\phi}}{\mathrm{d}r} \right)^2 + V_{\mathrm{eff}}(\hat{\phi}, T) \right\}$$

$$V_{\mathrm{eff}}^{(1)}(\hat{\phi}, T) = V_0 + V_{\mathrm{CW}} + \Delta V^{(1)}(T)$$

solution of the e.o.m. found by the path that minimizes the energy

Implementation via CosmoTransitions [Wainwright '12]

Dynamics of phase transitions

$$\Gamma \sim T^4 \left(\frac{\hat{S}_3}{2\pi T} \right)^{3/2} \exp\left(-\frac{\hat{S}_3}{T} \right)$$

High T $\Rightarrow$ classical motion in Euclidean space described by the action

$$\hat{S}_3 = 4\pi \int_0^\infty dr\, r^2 \left\{ \frac{1}{2} \left(\frac{d\hat{\phi}}{dr} \right)^2 + V_{\rm eff}(\hat{\phi}) \right\}$$

Field configuration as solutions to the e.o.m. found by the path that minimizes the energy

$$\begin{aligned}
V_{\rm eff}^{(1)}(\hat{\phi}) &= V_{\rm tree} + V_{\rm CW} + \Delta V^{(1)}(T) \\
V_{\rm CW} &= \sum_i (-1)^F n_i \frac{m_i^4}{64\pi^2} \left(\log\left[\frac{m_i^2(\hat{\phi}_\alpha)}{\Lambda^2} \right] - c_i \right) \\
\Delta V^{(1)}(T) &= \frac{T^4}{2\pi^2} \left\{ \sum_b n_b J_B \left[\frac{m_b^2(\hat{\phi}_\alpha)}{T^2} \right] - \sum_f n_f J_F \left[\frac{m_f^2(\hat{\phi}_\alpha)}{T^2} \right] \right\}
\end{aligned}$$

Loop and thermal corrections in then effective potential

Conclusions

The multi-messenger perspective applied to distinguish DM models

GW spectra to characterize and study different EoS for different DM candidates

Different seesaw variants lead to distinct GW spectra!

Gravitational wave to shed light on the mystery of DM & neutrino mass generation!

谢谢

Tack!

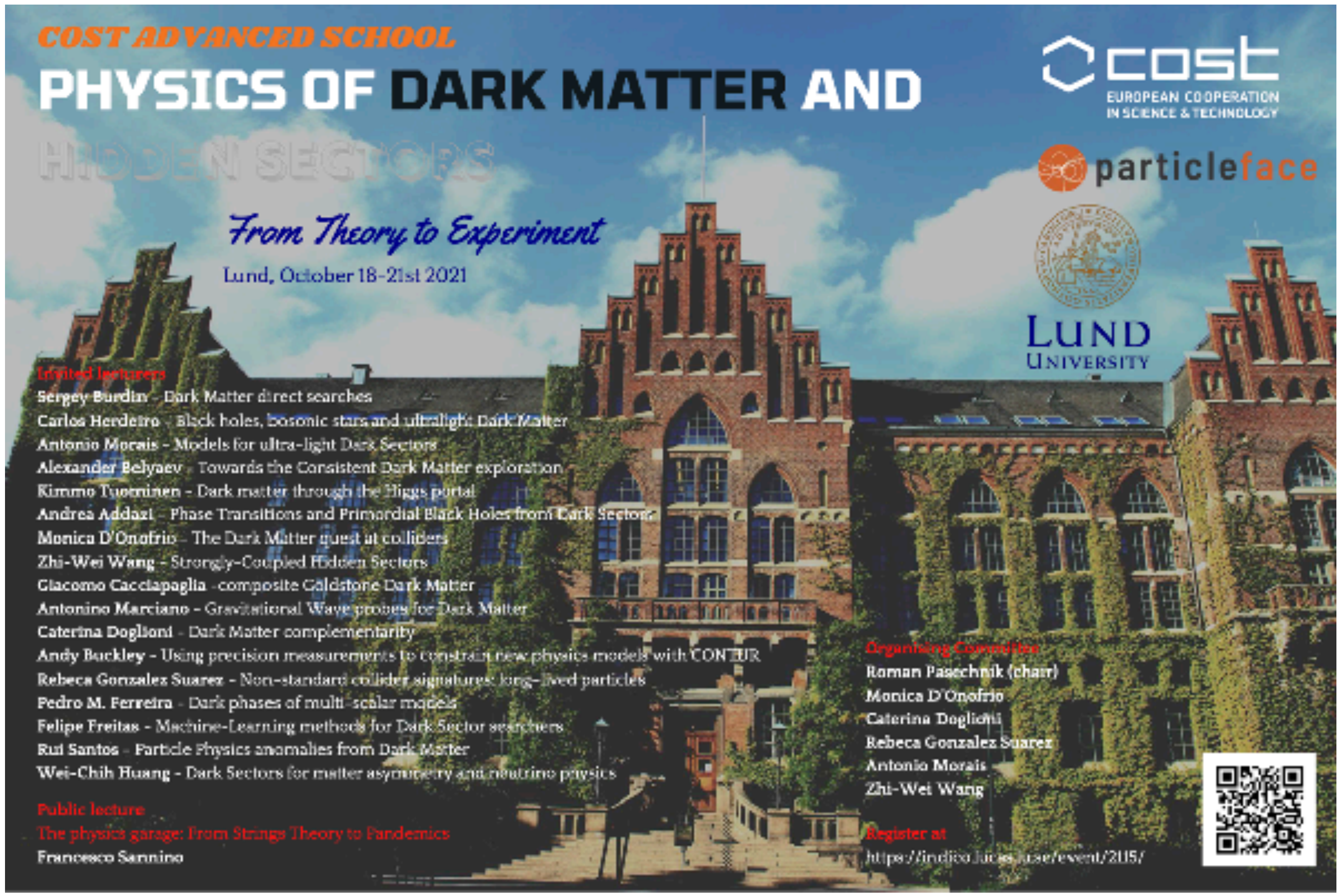

Thank you!

Grazie!

Neutrino physics and the mass-generation

Standard Type-I models (high scale)

$$\mathcal{L}_{\text{Yuk}}^{\text{Type-I}} = Y_\nu \bar{L} H \nu^c + M \nu^c \nu^c + h.c.$$

$L = (\nu, l)^T$ and ν^c three RH-neutrinos colored as SM-singlet

Y_ν and M 3 x 3 matrices

M explicitly break lepton number symmetry $U(1)_L \to \mathbb{Z}_2$

Mass for light neutrinos generated by EWSB $m_\nu \sim \mathcal{O}(0.1\text{eV})$

$$m_\nu^{\text{Type-I}} = \frac{v_h^2}{2} Y_\nu^T M^{-1} Y_\nu \qquad \langle H \rangle = \frac{v_h}{\sqrt{2}} \qquad Y_\nu \sim \mathcal{O}(1) \qquad M \sim O(10^{14}\text{GeV})$$

Inverse see-saw (low scale)

Two additional gauge singlet fermions, with opposite lepton number charge ν^c, S

$$\mathcal{L}_{\text{Yuk}}^{\text{Inverse}} = Y_\nu \bar{L} H \nu^c + M \nu^c S + \mu S S + \text{h.c.}$$

The smallness of the neutrino mass is linked to the breaking $U(1)_L \to \mathbb{Z}_2$

This is triggered by the μ-term $m_\nu^{\text{Inverse}} = \frac{v_h^2}{2} Y_\nu^T M^{T^{-1}} \mu \, M^{-1} Y_\nu$

Small neutrino masses are protected by $U(1)_L$ (restored for $\mu \to 0$)

Introducing the Majoron

Global B-L spontaneously broken by a SM complex scalar singlet and generation of LH neutrino mass

The NGB associated to the symmetry is the Majoron

Possible detection in neutrinoless double-beta decays (GERDA, EXO)

The effective action for the Majoron

$$\mathcal{L}_M = f H \bar{L} \nu_R + h \sigma \bar{\nu}_R \nu_R^c + h.c. + V(\sigma, H)$$

A complex singlet scalar σ, **the majoron**, with *L* (σ) = −2

$$V(\sigma, H) = V_0(\sigma, H) + V_1(\sigma) + V_2(h, \sigma)$$

$$V_0(\sigma, H) = \lambda_s \left(|\sigma|^2 - \frac{v_{BL}^2}{2} \right)^2 + \lambda_H \left(|H|^2 - \frac{v^2}{2} \right)^2 + \lambda_{sH} \left(|\sigma|^2 - \frac{v_{BL}^2}{2} \right) \left(|H|^2 - \frac{v^2}{2} \right) ,$$

$$V_1(\sigma) = \frac{\lambda_1}{\Lambda} \sigma^5 + \frac{\lambda_2}{\Lambda} \sigma^* \sigma^4 + \frac{\lambda_3}{\Lambda} (\sigma^*)^2 \sigma^3 + h.c.$$

$$V_2(H, \sigma) = \beta_1 \frac{(H^\dagger H)^2 \sigma}{\Lambda} + \beta_2 \frac{(H^\dagger H) \sigma^2 \sigma^*}{\Lambda} + \beta_3 \frac{(H^\dagger H) \sigma^3}{\Lambda} + h.c. .$$

The effective action for the Majoron

$$
\begin{aligned}
V_1^{(6)}(\sigma) = & \frac{\gamma_1}{\Lambda^2}\sigma^6 + \frac{\gamma_2}{\Lambda^2}\sigma^*\sigma^5 + \frac{\gamma_3}{\Lambda^2}(\sigma^*)^2\sigma^4 \\
& + \frac{\gamma_4}{\Lambda^2}(\sigma^*)^3\sigma^3 + h.c. \, , \\
V_2^{(6)}(\sigma, H) = & \frac{\delta_1}{\Lambda^2}(H^\dagger H)^2\sigma^2 + \frac{\delta_2}{\Lambda^2}(H^\dagger H)^2\sigma^*\sigma \\
& + \frac{\delta_3}{\Lambda^2}(H^\dagger H)\sigma^3\sigma^* + \frac{\delta_4}{\Lambda^2}(H^\dagger H)(\sigma\sigma^*)^2 \\
& + \frac{\delta_5}{\Lambda^2}(H^\dagger H)\sigma^4 + h.c. \, .
\end{aligned}
$$

Missing energy channel and LHC data

$$\Gamma(H \to \chi\chi) = \frac{C^2_{h\chi\chi} v^2}{64\pi m_H}\sqrt{1 - \frac{m_\chi^2}{m_H^2}}$$

$$C_{H\chi\chi} = \lambda_{H\chi\chi} + \frac{\beta_2}{\Lambda} v_\sigma.$$

$$Br(H \to invisible) = \frac{\Gamma_{inv}}{\Gamma_{inv} + \Gamma_{SM}} < 0.51\,(95\%\,\text{C.L.})$$

channel	ATLAS	CMS	ATLAS+CMS
$\mu_{\gamma\gamma}$	$1.15^{+0.27}_{-0.25}$	$1.12^{+0.25}_{-0.23}$	$1.16^{+0.20}_{-0.18}$
μ_{WW}	$1.23^{+0.23}_{-0.21}$	$0.91^{+0.24}_{-0.21}$	$1.11^{+0.18}_{-0.17}$
μ_{ZZ}	$1.51^{+0.39}_{-0.34}$	$1.05^{+0.32}_{-0.27}$	$1.31^{+0.27}_{-0.24}$
$\mu_{\tau\tau}$	$1.41^{+0.40}_{-0.35}$	$0.89^{+0.31}_{-0.28}$	$1.12^{+0.25}_{-0.23}$
μ_{bb}	$0.62^{+0.37}_{-0.36}$	$0.81^{+0.45}_{-0.42}$	$0.69^{+0.29}_{-0.27}$

$$\mu_F = \frac{\sigma^{NP}(pp \to H)}{\sigma^{SM}(pp \to H)} \frac{BR^{NP}(H \to F)}{BR^{SM}(H \to F)}$$

Majoron phenomenology

Cosmological limits very stringent on SSB scales beyond EW phase-transition

Very open limits on smaller scales!

Possibility to say something about the nature of the phase transition: violent Majoron, with FOPT

A. Addazi & A. Marciano, CPC (2018), arXiv:1705.08346

FOPT at 10 GeV

A. Addazi & A. Marciano, CPC (2018), arXiv:1705.08346

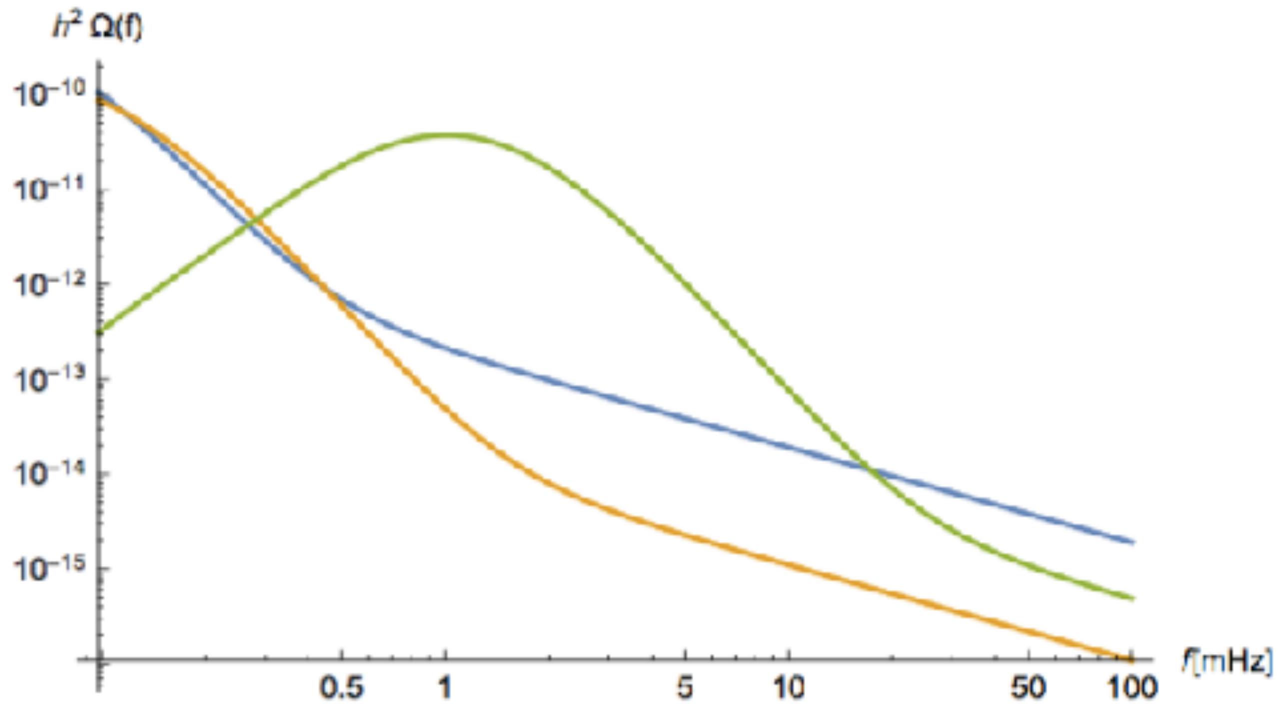

FIG. 1. The gravitational waves energy density as a function of the frequency is displayed. We use the same model independent parametrization of Ref.[18]. We show three *non-runnaway* bubbles cases which are compatible with the B-L first order phase transition: In blue, we consider the case of $\bar{T} = 50\,\mathrm{GeV}$, $\beta/\bar{H} = 100$, $\alpha = 0.5$, $\alpha_\infty = 0.1$, $V_B = 0.95$; in green $\bar{T} = 20\,\mathrm{GeV}$, $\beta/\bar{H} = 10$, $\alpha = 0.5$, $\alpha_\infty = 0.1$, $V_B = 0.95$. Orange: $\bar{T} = 10\,\mathrm{GeV}$, $\beta/\bar{H} = 10$, $\alpha = 0.5$, $\alpha_\infty = 0.1$, $V_B = 0.3$. The three cases lies in the sensitivity range of LISA [18].

Constrained from GW, colliders and cosmology

A. Addazi & A. Marciano, CPC (2018), arXiv:1705.08346

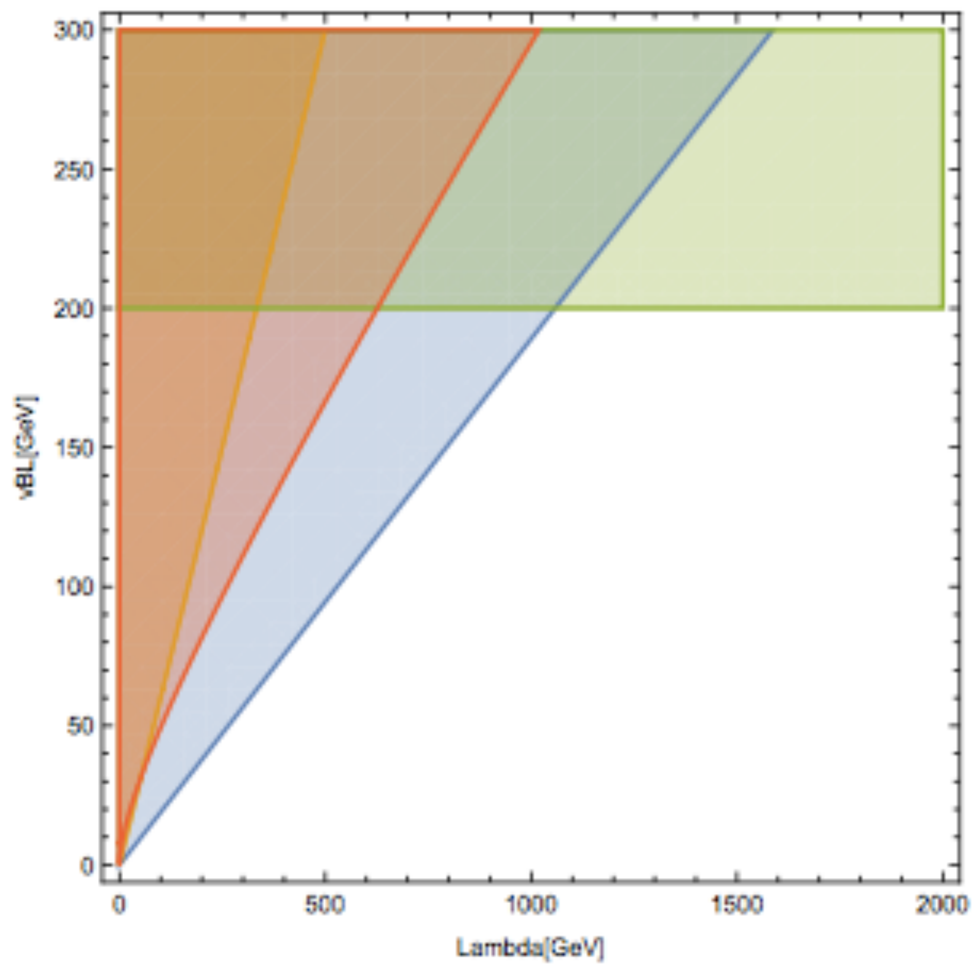

FIG. 2. We report the limits from LHC and future CEPC (in brown and blu respectively), cosmological sphaleron bounds (green) and the region which will be probed by eLISA (red). The case of $\beta_2 = 1$ is displayed.

Constrained from radio telescopes at KeV scales

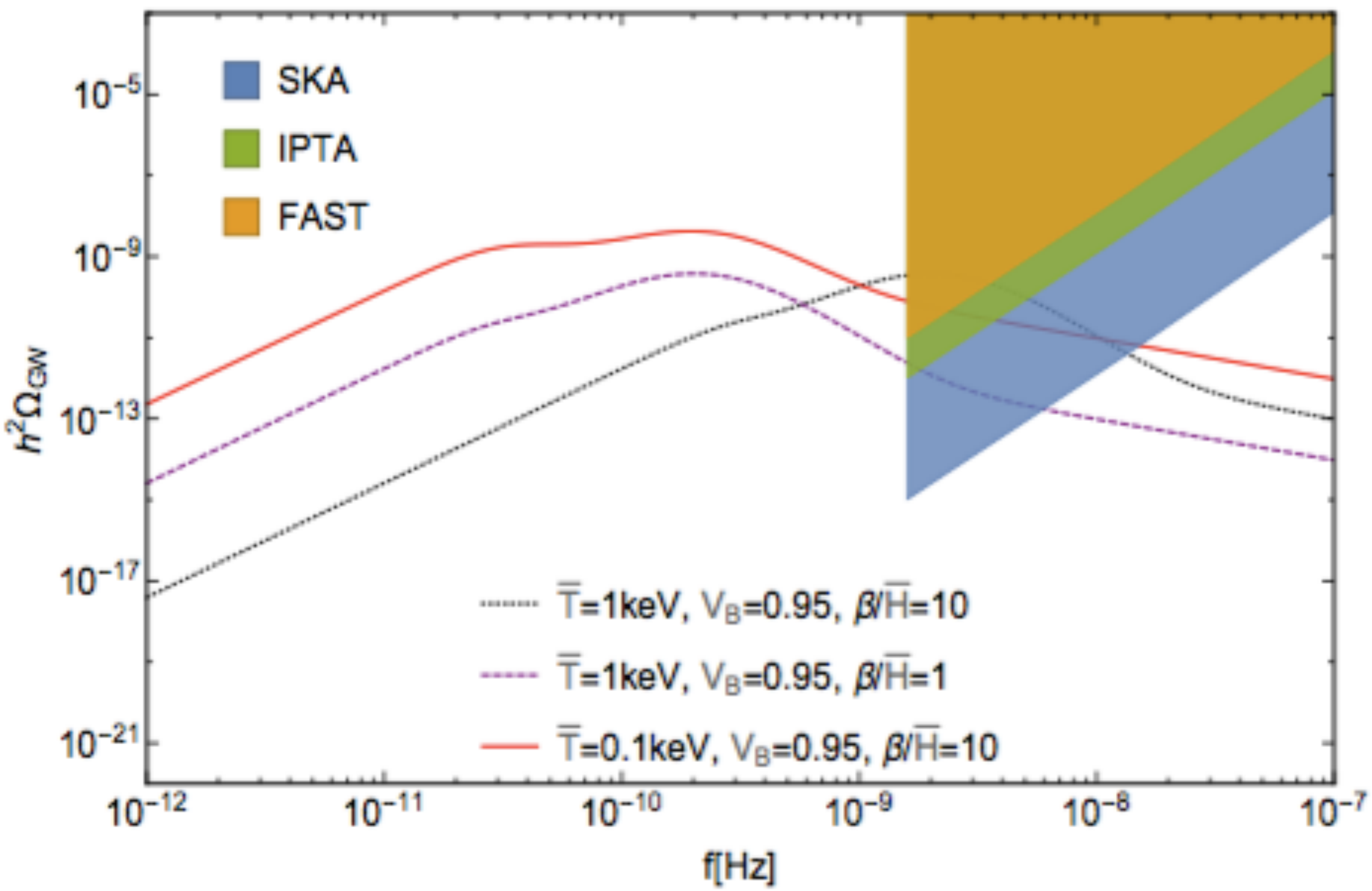

Type-I and Inverse See-saw with Majoron

For the majoron, $L(\sigma) = -2$ and mass terms read now:

$M\nu^c\nu^c \to Y_\sigma \sigma \nu^c \nu^c$ (type-I variant) $\mu SS \to Y_\sigma \sigma SS$ (low-scale inverse variant)

$\langle\sigma\rangle = \frac{v_\sigma}{\sqrt{2}}$ breaks spontaneously $U(1)_L \to \mathbb{Z}_2$

$M \to Y_\sigma v_\sigma/\sqrt{2}$ (type-I variant) $\mu \to Y_\sigma v_\sigma/\sqrt{2}$ (low-scale inverse variant)

Extended scalar sector:

$$V_0 = V_{\mathrm{SM}} + \mu_\sigma^2 \sigma^* \sigma + \lambda_\sigma (\sigma^* \sigma)^2 + \lambda_{h\sigma} H^\dagger H \sigma^* \sigma + \left(\tfrac{1}{2}\mu_b^2 \sigma^2 + \mathrm{c.c.}\right)$$

Tiny $U(1)_L$ soft breaking term $\mu_b \sim \mathcal{O}(1\mathrm{KeV})$

Resulting pseudo-Goldstone boson as testable DM candidate (Valle et '93, '07)

See-saw mechanism and GW production

See-saw gravitational footprint

High scale type-I seesaw with explicit U(1)$_L$ violation

$$\mathcal{L}_{\rm Yuk}^{\rm Type-I} = Y_\nu \bar{L} H \nu^c + M \nu^c \nu^c + h.c.$$

Heavy isosinglet neutrinos decouple from EW-scale: no FOPT and thus no GW signal from EWPT!

Low-scale inverse seesaw with explicit U(1)$_L$ violation

$$\mathcal{L}_{\rm Yuk}^{\rm Inverse} = Y_\nu \bar{L} H \nu^c + M \nu^c S + \mu S S + \text{h.c.}$$

Singlets closer to EW scale and sizable Higgs coupling

Thermal corrections from heavy neutrinos induce FOPT

Fermions affect PT at loop level, enabling weak FOPT only

Y_ν	M/GeV	generations
[0.2, 3.0]	[50, 500]	[3, 30]

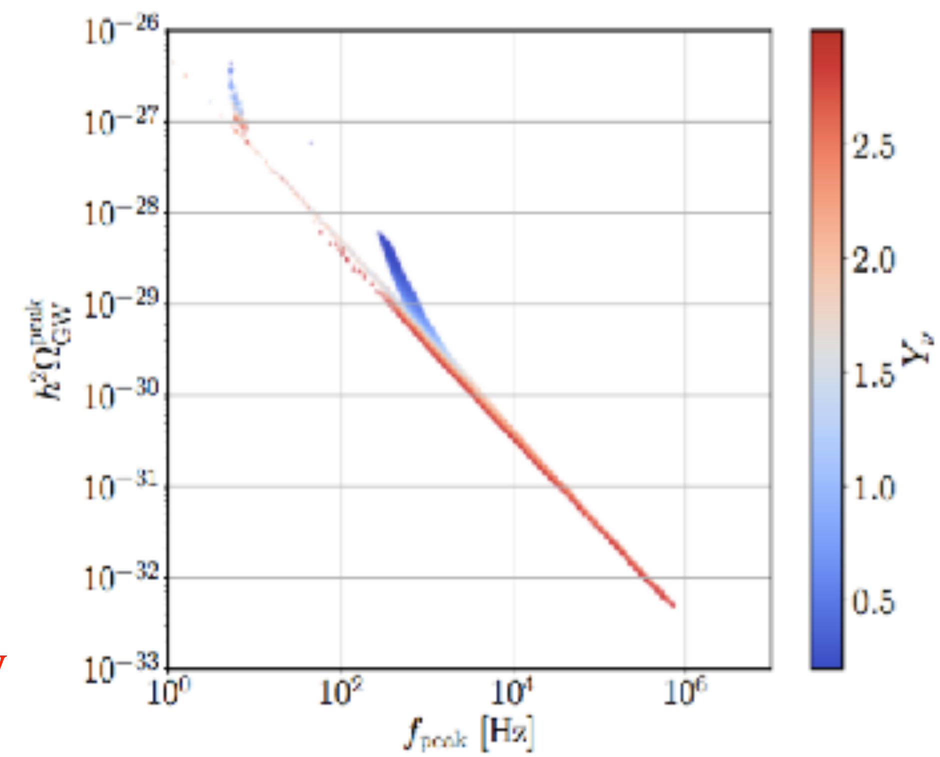

Signal below current and forthcoming instrumental sensitivity!

Gravitational footprint of Lepton number SSB

Spontaneous breaking of $U(1)_L \to Z_2$ and inverse see-saw mechanism

Type-I variant

$$\boxed{M\nu^c\nu^c \to Y_\sigma \sigma \nu^c \nu^c}$$

Low-scale inverse variant

$$\boxed{\mu SS \to Y_\sigma \sigma SS}$$

Majoron scalar σ responsible for a new richer pattern of FOPTs

Inverse See-Saw with Majoron

Strength of PT enhanced by tree-level contributions

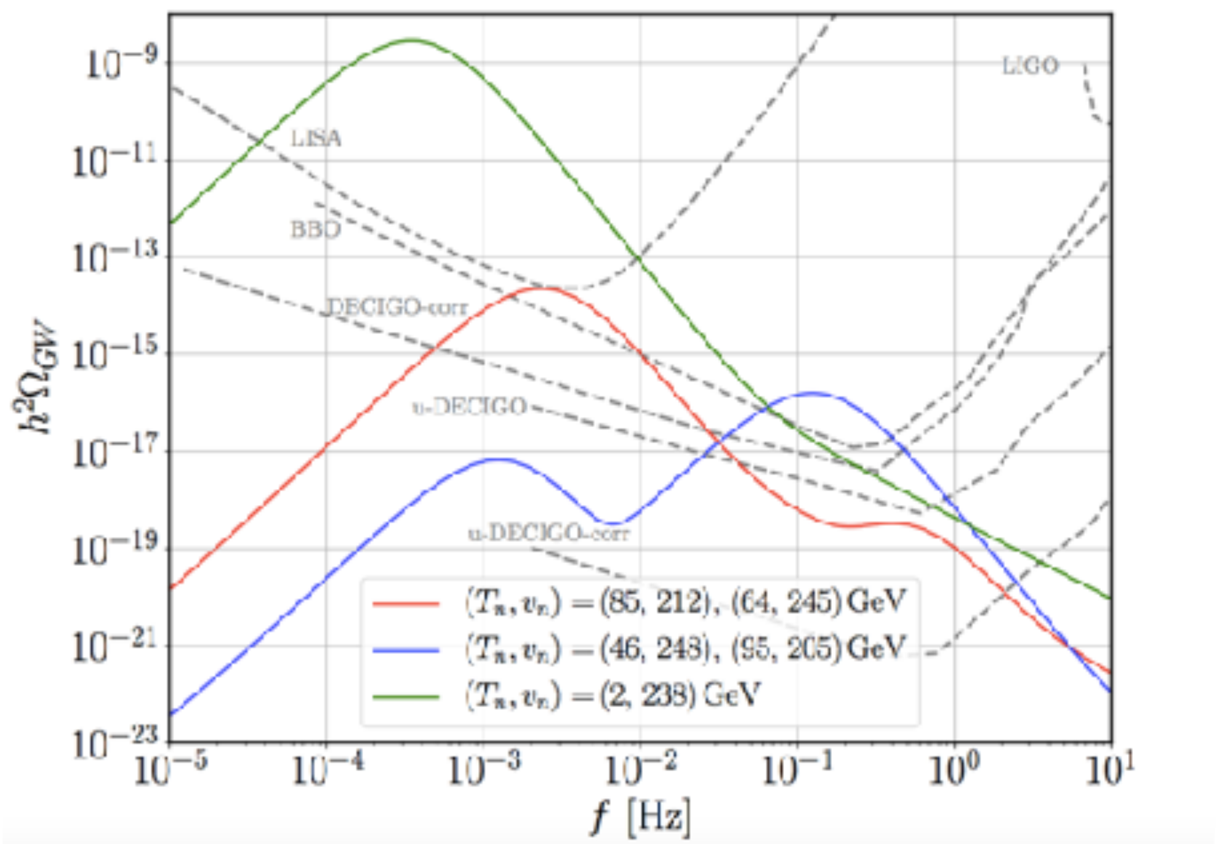

Characteristic signal with multi-peak scenario!

Richer patterns of FOPTs

Not only heavy isosinglet fermions couple to the Higgs → the Majoron complex scalar that breaks spontaneously $U(1)_L$ can couple substantially to the Higgs

↓

Generation of two or three GW peaks

At the end of any FOPT scalar potential minimization requires non vanishing VEVs to be associated with the generation of EW and neutrino mass scales

Class I) $(0,0) \to (v_H, v_\sigma)$

Class II)

$(0,0) \to (v_H, 0) \to (v_H, v_\sigma)$ for $v_\sigma < v_H$

$(0,0) \to (0, v_\sigma) \to (v_H, v_\sigma)$ for $v_\sigma > v_H$

Class III)

$(0,0) \to (v_H, 0) \to (0, v_\sigma) \to (v_H, v_\sigma)$ for $v_\sigma < v_H$

$(0,0) \to (0, v_\sigma) \to (v_H, 0) \to (v_H, v_\sigma)$ for $v_\sigma > v_H$

Three possible scenarios

Three possible scenarios, with nearly preserved U(1)L, namely $v\sigma$ ($T = 0$) ~ O (1 keV)

Peak Id	$(v_h^i, v_\sigma^i) \rightarrow (v_h^f, v_\sigma^f)$	α	β/H
Green 1	$(249, 0) \rightarrow (238, 0)$	16.0	715
Red 1	$(0, 70.7) \rightarrow (212, 0)$	8.83×10^{-2}	109
Red 2	$(228, 0) \rightarrow (245, 0)$	6.85×10^{-3}	2.31×10^4
Blue 1	$(0, 98.9) \rightarrow (205, 0)$	5.72×10^{-2}	5.08×10^3
Blue 2	$(239, 0) \rightarrow (248, 0)$	3.73×10^{-3}	86.7

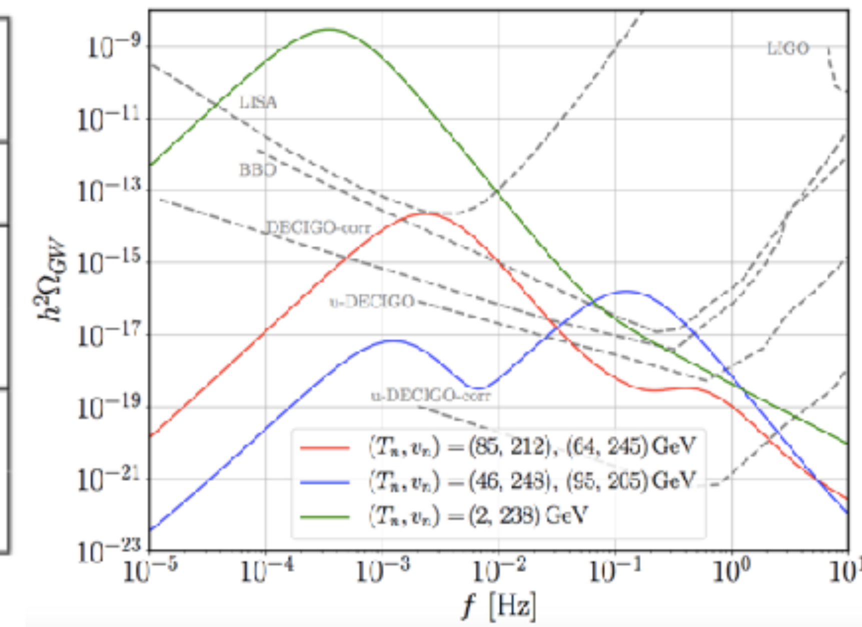

Curve	m_{σ_R}/GeV	$\lambda_{\sigma h}$	λ_σ	M_ν/GeV	Y_σ
Green	68.9	3.56	7.86×10^{-3}	147	4.83
Red	439	7.42	8.48	324	2.71
Blue	378	5.08	1.67	303	0.126

Detectable by **LISA**: very strong FOPT with $v_n/T_n = 119$

(Consistent with invisible Higgs decays LHC bounds [Bonilla, Romão, Valle (2016)])

Two-peak scenarios detectable by DECIGO

Large quartic couplings enhance m/T and facilitate these scenarios: Bosonic $(m/T)^3$ contributions in $\Delta V^{(1)}$ (T) produce potential barriers

Multi-peak scenarios and generic features

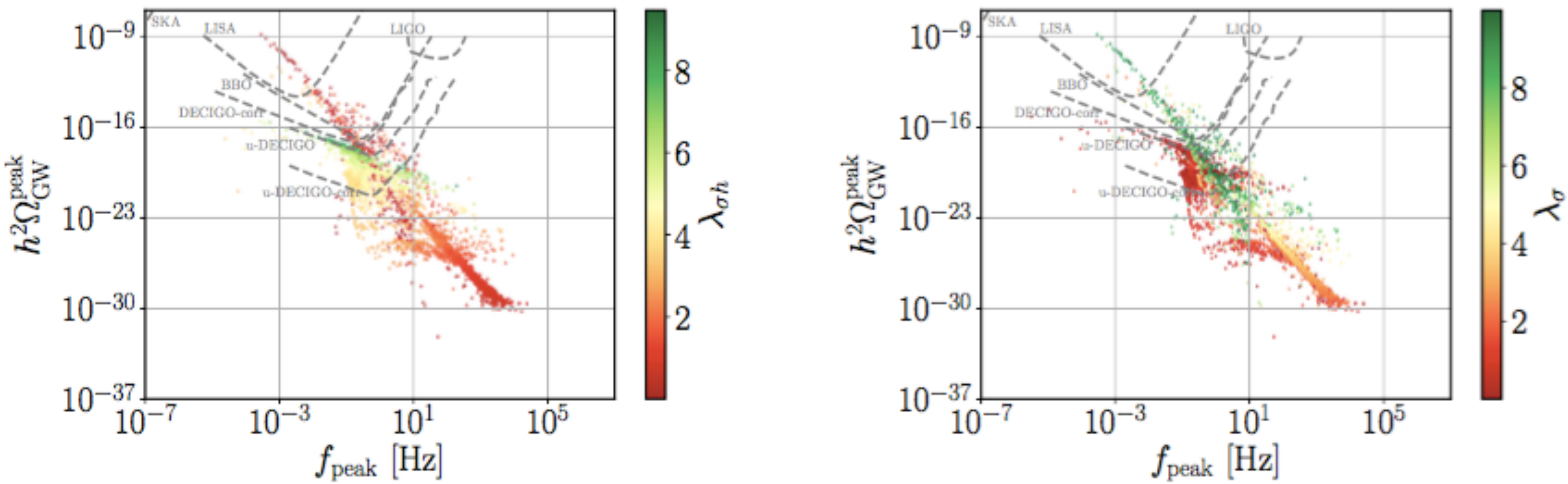

At least one quartic coupling involving σ is sizable

Multi-peak feature as a prediction of the Inverse seesaw with Majoron

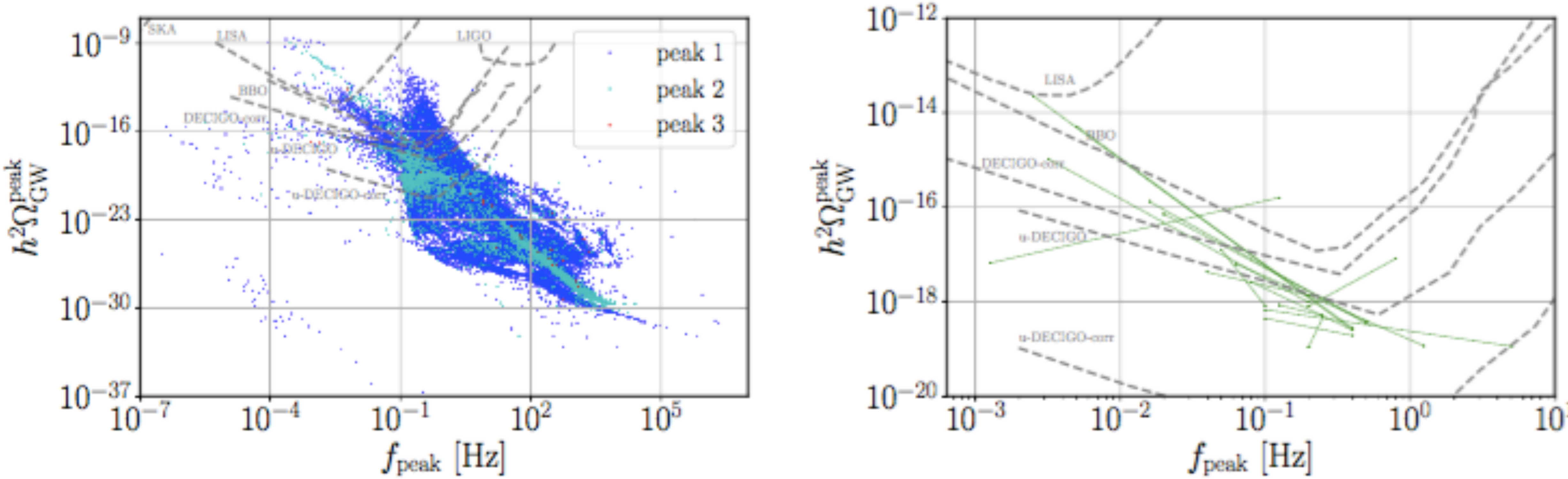

Very hard to resolve the third peak

Multi-peaks only due to distinct phase transitions (no competition effect from the three mechanism, i.e. collision, sound waves, turbulence)

Possibility to distinguish/falsify neutrino mass generation mechanism

Type-I seesaw with Majoron

High scale variant: $Y_\nu \sim \mathcal{O}(1) \to M = Y_\sigma \nu_\sigma/\sqrt{2} \sim \mathcal{O}(10^{14}\text{GeV})$

for $Y_\sigma \sim \mathcal{O}(1)$ then $\nu_\sigma \sim \mathcal{O}(10^{14}\text{GeV}) \to$ NO FOPT

Low scale variant: $Y_\nu \sim \mathcal{O}(10^{-6}) \to M = Y_\sigma \nu_\sigma/\sqrt{2} \sim \mathcal{O}(100\text{GeV})$

new states do not decouple: FOPT and GW are found

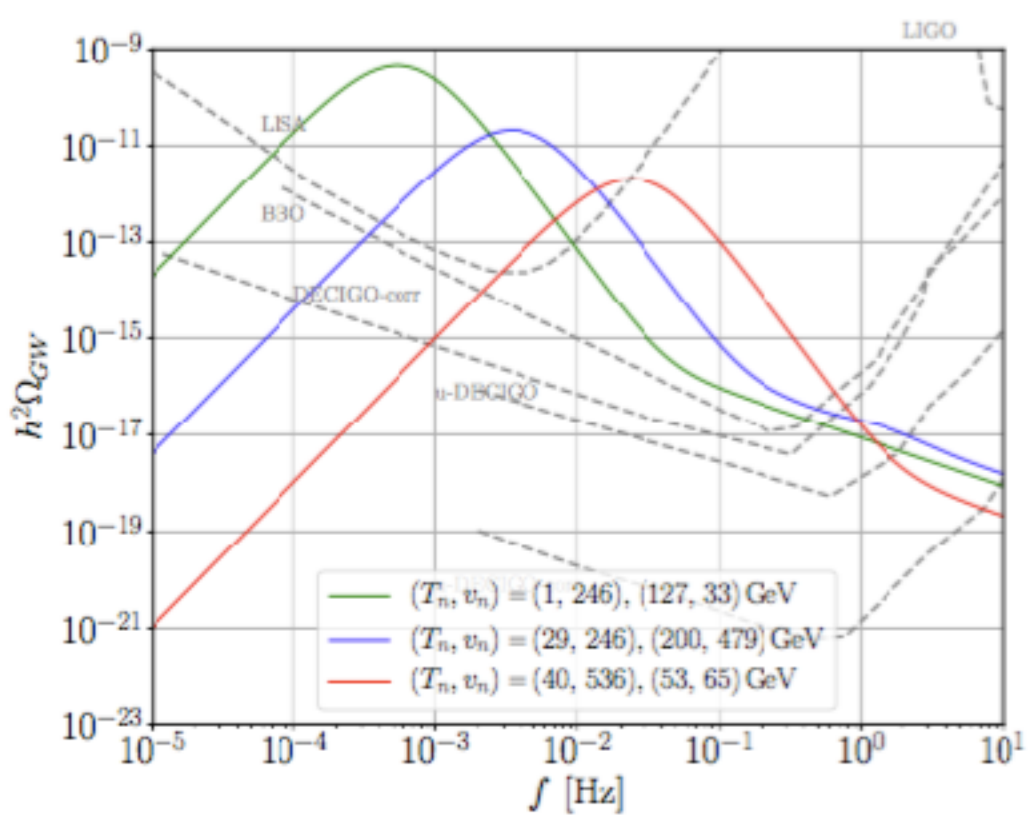

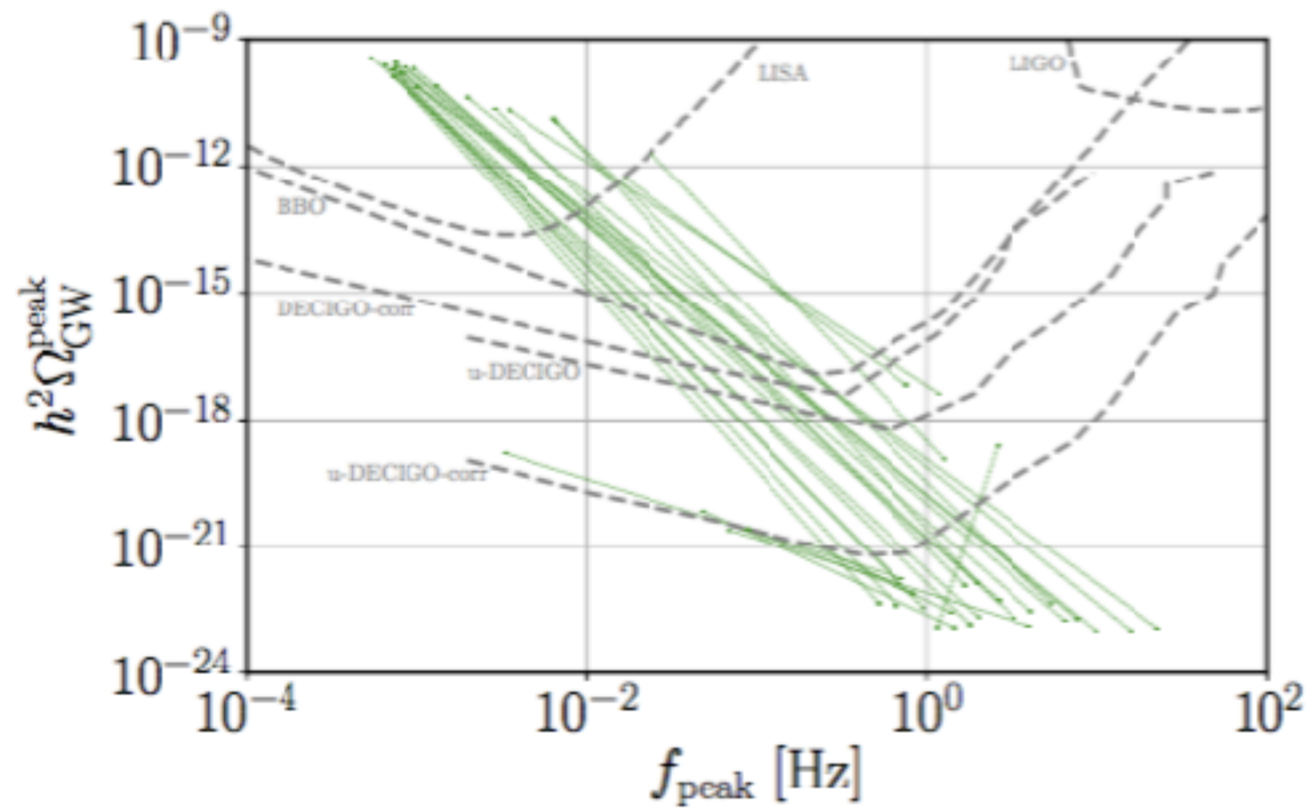

Less double peaks than in the Inverse See-Saw case, and mainly out of reach

Double-peak within experimental reach much rarer

In contrast to inverse seesaw + majoron one, PT is typically much stronger hiding the smaller peak

Curve	m_{h_2}/GeV	λ_h	$\lambda_{\sigma h}$	λ_σ	$\cos\theta$	$v_\sigma(T=0)$	M_ν/GeV	Y_σ
Green	83.1	0.0624	0.310	8.16	0.962	30.3	456	2.08
Red	793	0.389	0.594	0.350	0.974	924	90.5	2.59
Blue	334	0.265	0.332	0.243	0.913	449	57.8	2.97

Peak Id	$(v_h^i, v_\sigma^i) \to \left(v_h^f, v_\sigma^f\right)$	α	β/H	$f_{\mathrm{peak}}/\mathrm{Hz}$
Green 1	$(0, 45.4) \to (33.4, 45.1)$	6.39×10^{-4}	2.36×10^4	0.955
Green 2	$(246, 30.8) \to (246, 29.7)$	6.70	3.50×10^3	5.37×10^{-4}
Red 1	$(0, 967) \to (64.8, 964)$	1.20×10^{-2}	8.16×10^4	1.26
Red 2	$(213, 935) \to (536, 750)$	0.249	2.68×10^3	0.0240
Blue 1	$(293, 305) \to (0, 479)$	1.30×10^{-2}	2.04×10^4	1.17
Blue 2	$(0, 554) \to (246, 450)$	0.632	574	3.48×10^{-3}

Second CP-even Higgs; $h = \cos\theta\, h_1 + \sin\theta\, h_2$

Consistency with Higgs invisible decays bounds assured